Raman-Spektroskopie

W. Kiefer

Vortrag zur Lehrerfortbildung des

Physikalischen Instituts der

Universität Bayreuth

25. 10. 1978

Inhaltsverzeichnis

Literaturangaben:

1) J. Brandmüller und H. Moser, Einführung in die
   Ramanspektroskopie, Steinkopff-Verlag, Darmstadt 1962

2) H.A. Szymanski, Raman Spectroscopy, Vol. 1+2,
   Plenum Press, New York 1967

3) A. Anderson, The Raman Effect, Vol. I and II
   Marcel Dekker, New York 1973

4) S.K. Freeman, Applications of Laser Raman Spectroscopy
   John Wiley & Sons, New York 1974

5) R.J.H. Clark and R.E. Hester, Advances in Infrared and
   Raman Spectroscopy, Vol. 1-5
   Heyden, London 1975-1978

6) D.A. Long, Raman Spectroscopy
   McGraw-Hill 1977

7) H. Siebert, Anwendungen der Schwingungsspektroskopie
   in der anorganischen Chemie, Springer-Verlag, Berlin 1966

Raman-Spektroskopie

A. Einleitung

Vor genau 50 Jahren gelang dem 1970 verstorbenen indischen Physiker Sir Chandrasekhara Venkata Raman der experimentelle Nachweis eines fünf Jahre vorher von dem österreichischen Physiker Gustav Adolf Smekal vorhergesagten Effekts, des Raman-Effekts. Raman erhielt im Jahre 1930 für diese Entdeckung den Nobelpreis.

Der Raman-Effekt ist eine der vielen Erscheinungen, die bei Wechselwirkung von Licht mit Materie auftreten. Und zwar handelt es sich darum, daß das von im allgemeinen regellos angeordneten Molekülen, die mit diskontinuierlichem, im einfachsten Fall monochromatischem Licht der Frequenz ν_0 bestrahlt werden, in den Raum gestreute Licht nicht mehr die gleiche spektrale Zusammensetzung hat, sondern außer der Primärfrequenz noch weitere Spektrallinien mit den Frequenzen $\nu_1, \nu_2, \nu_3, \ldots, \nu_i$ aufweist. Die Frequenz<u>differenzen</u> zwischen der "Erregerlinie ν_0". und den "verschobenen" oder "Ramanlinien ν_i", also $\Delta\nu_i = \nu_i \pm \nu_0$ erweisen sich als abhängig von der Struktur des streuenden Moleküls und sind nichts anderes als jene, unter Umständen auch in ultraroter Absorption beobachtbaren Frequenzen, die einerseits den Schwingungen, die die Atome des Moleküls gegeneinander ausführen können, andererseits den Rotationen des Gesamtmoleküls, zukommen.

Ist $\nu_i < \nu_0$, ν_i also gegen den "roten" Spektralbereich mit kleinerer Frequenz ν und größerer Wellenlänge λ verschoben, dann spricht man von "Stokes'scher Raman-Streuung"; für "blau-verschobene" Streustrahlung (anti-Stokes) muß $\nu_i > \nu_0$ sein. Die Erregerlinie ν_0 selbst wird als "unverschoben" gestreute oder auch als "Rayleigh"-Linie bezeichnet. Die klassische Streutheorie deutet das Auftreten der frequenzverschobenen Linien als eine Modulation der eingestrahlten Lichtwelle mit den Schwingungen der Atome eines Moleküls, bzw. mit der Rotation des ganzen Moleküls, oder im Festkörper mit Kristallgitterschwingungen.

Bis vor etwa fünfzehn Jahren konnte man Raman-Spektren praktisch nur von mehreren Gramm farbloser flüssiger Stoffe erhalten. Die Erregung der Spektren erfolgte fast ausschließlich mit Linien von Quecksilberlampen. Die Entdeckung des Lasers im Jahre 1960 durch T.H. Maiman leitete bald danach eine Renaissance der Ramanspektroskopie ein. Die heute verfügbaren Laser-Lichtquellen liefern eine spektrale Strahlungsdichte, die um ca. zehn Zehnerpotenzen höher ist als die der früher benutzten Quecksilber-Dampflampen. Im gleichen Maße wie die spektrale Strahlungsdichte der Lichtquelle, steigt die Strahlungsdichte der Ramanstrahlung einer Probe. Die Laser-Lichtquellen haben die experimentelle Situation völlig verändert. Die erforderlichen Probenmengen liegen jetzt im Milli- und Mikrogrammbereich. Gase, Flüssigkeiten und feste Stoffe, insbesondere luftempfindliche und aggressive Proben, Einkristalle, Kristallnadeln und Fasern sowie wäßrige Lösungen lassen sich untersuchen. Identifizierungen und Strukturaufklärungen von Molekülen, biochemische Analysen und Analysen im Umweltschutz sind wichtige Anwendungen der Raman-Spektroskopie. Sie ist jetzt ein leistungsfähiger Partner der übrigen Methoden der instrumentellen Analyse. In der Physik eröffneten sich neue Möglichkeiten, wie z.B. die inelastische Lichtstreuung an Phononen, Polaritonen, Magnonen, Plasmonen, Magnaritonen, Plasmaritonen, etc.

B. Klassische Theorie des Ramaneffekts

Die Raman-Spektren entstehen durch Wechselwirkung von Lichtquanten mit Molekülen. Lichtquanten besitzen die Eigenschaft von Teilchen und von Wellen. Daher ist die Wechselwirkung sowohl als Stoßprozeß eines Lichtquants mit einem Molekül, als auch als Modulation einer Welle durch die Schwingungen eines Moleküls zu verstehen.

Beim unelastischen Stoß eines Lichtquants mit einem Molekül kann die Schwingungsenergie vom Lichtquant auf das Molekül übertragen oder vom Molekül auf das Lichtquant abgegeben werden (Abb. 1 a). Die Anzahl der Moleküle im 1. angeregten Schwingungszustand N_s relativ zu der im Schwingungsgrundzustand N_o ist durch das Boltzmann-Gesetz gegeben (Abb. 1 b und 1 c) :

$$N_s = N_o \cdot e^{-h\nu_s / kT}$$

(1)

Bei 300° K und einer Schwingungsfrequenz von 1000 cm^{-1} befinden sich nur knapp 1% der Moleküle im 1. angeregten Zustand. Infolgedessen ist dann ein unelastischer Stoß eines Lichtquants mit einem Molekül, bei dem Schwingungsenergie an das Molekül abgegeben wird, ungefähr 100-mal so häufig, wie ein unelastischer Stoß, bei dem Schwingungsenergie vom Molekül an das Lichtquant abgegeben wird. Man beobachtet daher zweckmäßigerweise das intensivere Streuspektrum auf der langwelligen Seite der Erregerlinie (Abb. 1 d), das Stokes-Raman-Spektrum.

Die absolute Intensität der Schwingungsbande im Raman-Spektrum läßt sich durch Wechselwirkung des Moleküls mit einer elektromagnetischen Welle erklären. Bringt man ein Molekül in ein elektrisches Feld, so werden die positiven und negativen Ladungen etwas gegeneinander verschoben. Es entsteht ein induziertes Dipolmoment μ , dessen Größe proportional der einwirkenden elektrischen Feldstärke E und der Verschiebbarkeit der Ladungen im Molekül- der sog. Polarisierbarkeit α - ist:

$$\mu = \alpha E$$

(2)

Die Polarisierbarkeit eines Moleküls ist i.a. in Richtung der größten Ausdehnung eines Moleküls am größten. Man beschreibt die Richtungsabhängigkeit mit Hilfe der Komponenten α_{ij} (i, j = x,y,z), die den Polarisierbarkeitstensor bilden:

a) Einfallendes Photon $h\nu_0$ — Molekül ν_i — Gestreutes Photon $h\nu_{as} = h(\nu_0 + \nu_i)$; $h\nu_s = h(\nu_0 - \nu_i)$

b) E ; $h\nu_0$; $h\nu_s$; $h\nu_{as}$; N_s ; N_0

c) N ; N_0 ; $N_s = N_0 \cdot e^{-h\nu_s/KT}$; $T = 300\,K$; 0 ; 1000 ; $\tilde{\nu}\ [cm^{-1}] \longrightarrow$

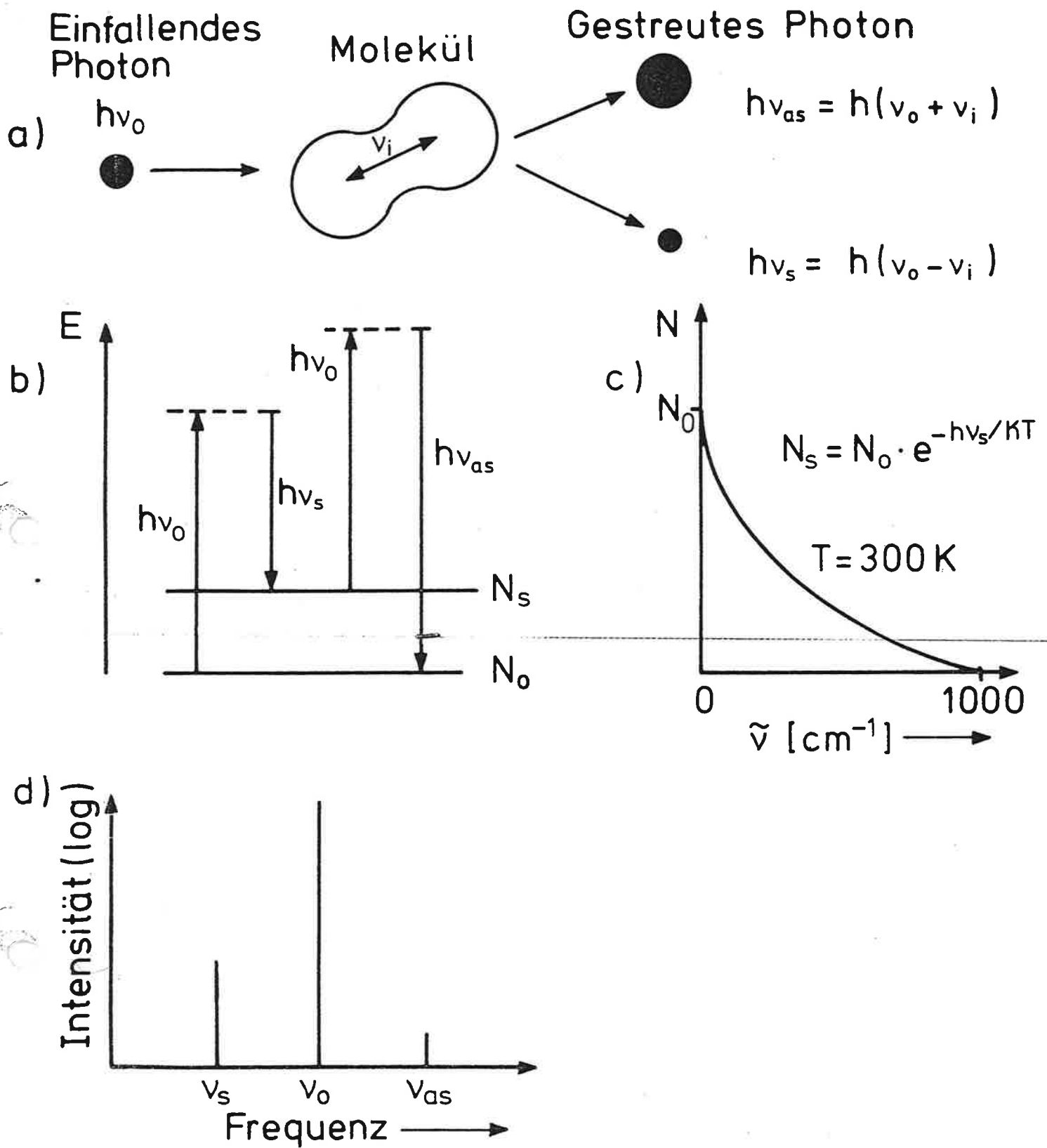d) Intensität (log) ; ν_s ; ν_0 ; ν_{as} ; Frequenz $\longrightarrow$

Abb. 1: Der Raman-Effekt als unelastischer Stoß Lichtquant-
Molekül. a) Stoßprozeß, b) Energieniveauschema, c)
relative Besetzung eines Schwingungsniveaus bei $\tilde{\nu}$
cm^{-1} und 300K, Stokes- und Anti-Stokes-Raman-Spektrum.

$$\mu_x = \alpha_{xx} E_x + \alpha_{xy} E_y + \alpha_{xz} E_z$$

$$\mu_y = \alpha_{yx} E_x + \alpha_{yy} E_y + \alpha_{yz} E_z$$

$$\mu_z = \alpha_{zx} E_x + \alpha_{zy} E_y + \alpha_{zz} E_z$$

(3)

Dieser Tensor ist im allgemeinen symmetrisch, d.h. $\alpha_{ij} = \alpha_{ji}$, er hat also nur sechs verschiedene Komponenten.

Wirkt ein elektrisches Wechselfeld auf das Molekül, so ändert sich auch das induzierte Dipolmoment mit dessen Frequenz ν_0. Das Molekül sendet dann (wie ein Hertzscher Dipol) Strahlung der gleichen Frequenz ν_0 aus. Führt das Molekül jedoch zusätzlich eine mechanische Schwingung aus, so werden die Bindungen dabei gestaucht, gedehnt oder gebogen. Dadurch verändert sich auch die elektrostatische Anziehung der Valenzelektronen durch die Kerne und damit deren Polarisierbarkeit. Infolgedessen wird sich die Amplitude der ausgesandten Welle im Rhythmus der mechanischen Schwingung des Moleküls ändern: Das Molekül sendet daher – wie ein Mittelwellensender – eine amplitudenmodulierte elektromagnetische Welle aus (Abb. 2).
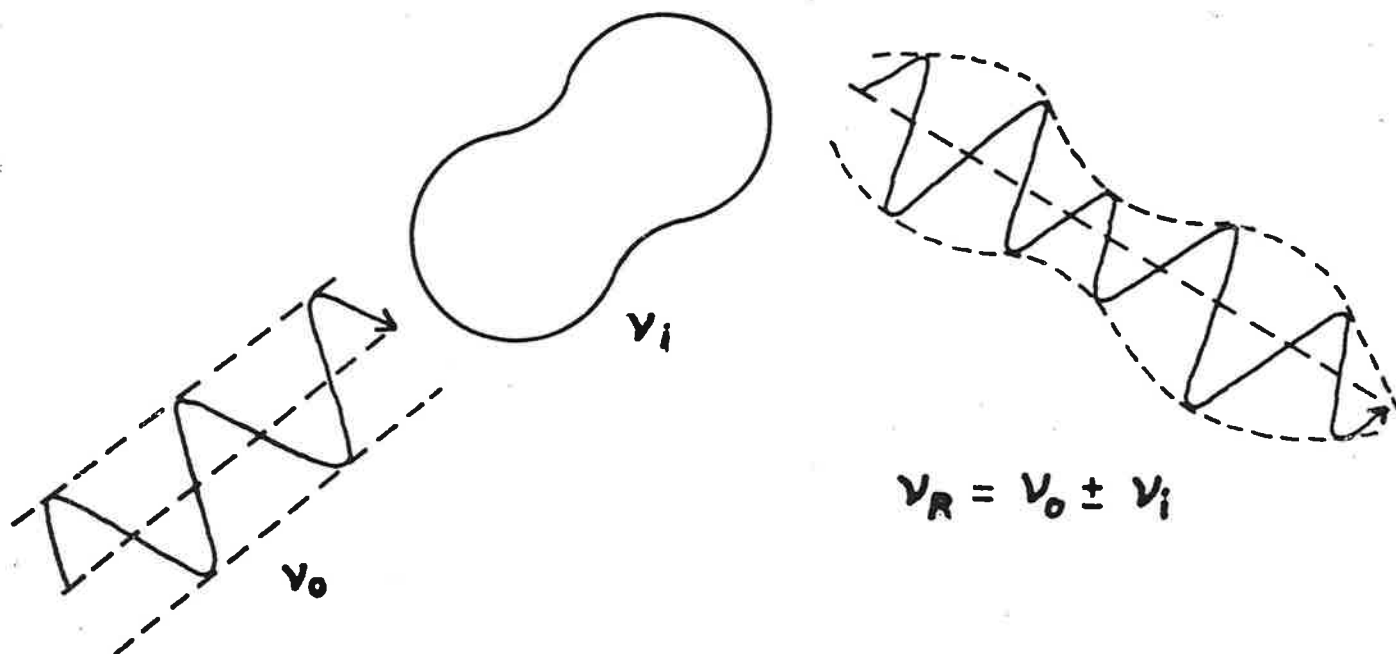

Abb. 2: Modulation der Streustrahlung eines schwingenden Moleküls.

Die klassische Theorie dafür ist: Die elektrische
Feldstärke der Erregerstrahlung ändert sich mit der Frequenz :

$$E = E_0 \cdot \cos 2\pi \nu_0 t \qquad (4)$$

Der Polarisierbarkeitstensor $\alpha = (\alpha_{ij})$ des Moleküls, das mit
der Frequenz ν_i mechanisch schwingt, setzt sich zusammen aus
einem unveränderten Anteil α_0 und einem Anteil, der sich mit
dieser Frequenz ν_i ändert:

$$\alpha = \alpha_0 + \left(\frac{\partial \alpha}{\partial Q_i}\right)_0 \cdot A_i \cos 2\pi \nu_i t \qquad (5)$$

$Q_i = A_i \cdot \cos 2\pi \nu_i t$ ist die Normalkoordinate, A_i beschreibt die
Amplitude der einzelnen Atome bei der Normalschwingung i. Aus
Gl. (4) und (5) ergibt sich für das induzierte Dipolmoment
$\mu = \alpha E$:

$$\mu = \alpha_0 E_0 \cos 2\pi \nu_0 t + \left(\frac{\partial \alpha}{\partial Q_i}\right)_0 A_i E_0 \cos(2\pi \nu_0 t) \cos(2\pi \nu_i t) \qquad (6)$$

Nach Anwendung der trigometrischen Additionstheoreme folgt
für das induzierte Dipolmoment eines Moleküls, das mit der
Frequenz ν_i mechanisch schwingt und das dabei einem Strahlungs-
feld der Frequenz ν_0 ausgesetzt ist:

$$\mu_i = \alpha_0 E_0 \cos(2\pi \nu_0 t) + \frac{1}{2} \left(\frac{\partial \alpha}{\partial Q_i}\right)_0 A_i E_0 \cdot$$
$$\cdot \left\{ \cos 2\pi (\nu_0 - \nu_i) t + \cos 2\pi (\nu_0 + \nu_i) t \right\} \qquad (7)$$

Der erste Term in Gl. (7) beschreibt die Rayleigh-Strahlung
mit der Frequenz ν_0 , der zweite die Stokes- ($\nu_0 - \nu_i$)
und Anti-Stokes-Raman-Strahlung ($\nu_0 + \nu_i$).

Die Intensität der Raman-Linien ist proportional dem
Quadrat der Änderung des induzierten Dipolmoments:

$$I_{Raman} \sim \overline{\ddot{\mu}^2} \qquad (8)$$

($\overline{}$ bedeutet zeitliche Mittelung)
und daher auch proportional dem Quadrat der Änderung der
Polarisierbarkeit, $\left(\frac{\partial \alpha}{\partial Q}\right)_0^2$, bei der Schwingung der Atome um
die Gleichgewichtslage.

Die Aussage der klassisch hergeleiteten Gl. (7), nach
der die Anti-Stokes- und die Stokes-Raman-Linie gleich intensiv
sein sollten, berücksichtigt noch nicht die unterschiedliche
Besetzung von Schwingungsgrundzustand und angeregtem
Schwingungszustand und steht noch im Widerspruch zur Beobachtung.
Die Quantenmechanik gibt die richtige Antwort.

Hiernach berechnet sich das Intensitätsverhältnis von
Anti-Stokes- zu Stokes-Raman-Linien :

$$\frac{I_{as}}{I_s} = \frac{(\nu_0 + \nu_i)^4}{(\nu_0 - \nu_i)^4} \cdot e^{-h\nu_i/kT} \qquad (9)$$

Zur Berechnung der Raman-Intensität für frei bewegliche Moleküle,
in Gasen oder Flüssigkeiten, benötigt man den Mittelwert $\bar{\alpha}$ und
die Anisotropie γ der Änderung der Polarisierbarkeit bei der
Normalschwingung i:

$$\bar{\alpha} = \frac{1}{3} (\alpha_{xx} + \alpha_{yy} + \alpha_{zz}) \qquad (10)$$

$$\gamma^2 = \frac{1}{2} \left\{ (\alpha_{xx} - \alpha_{yy})^2 + (\alpha_{yy} - \alpha_{zz})^2 + (\alpha_{zz} - \alpha_{xx})^2 + \right. $$
$$\left. + 6 (\alpha_{xy}^2 + \alpha_{yz}^2 + \alpha_{zx}^2) \right\} \qquad (11)$$

Strahlt man nach Abb. 3 in die Substanzküvette polarisiertes
Erregerlicht in Richtung der c-Achse ein und beobachtet man -
ohne Analysator - die Raman-Strahlung in Richtung der b-Achse,
so muß man zweierlei Intensitäten berücksichtigen:

$I_\parallel$: für Erregerstrahlung mit dem elektrischen Vektor
parallel zur Richtung der Polarisation des einfallenden
Laserstrahls (Richtung a)

$I_\perp$: für Erregerstrahlung mit dem elektrischen Vektor senk-
recht zur Richtung der Polarisation des einfallenden
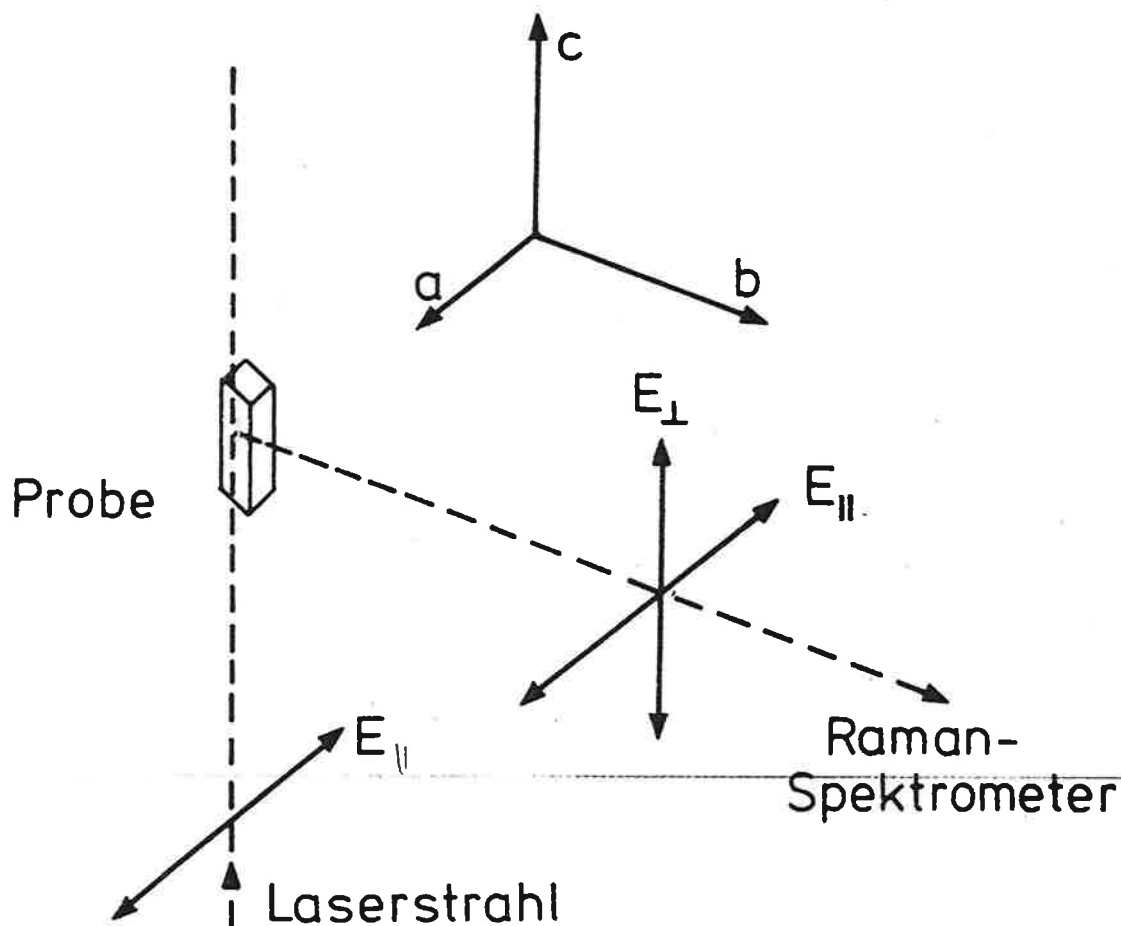Laserstrahles, also parallel der c-Achse:

<u>Abb. 3</u>: Messung des Depolarisationsgrades der Raman-Strahlung
bei Anwendung eines Laser-Strahles als Erregerstrahlung

$$I_{\shortparallel} \sim \left(\bar{\alpha}^2 + \frac{7}{45}\gamma^2 \right) \qquad (12)$$

$$I_{\perp} \sim \frac{6}{45}\gamma^2 \qquad (13)$$

Das Verhältnis beider Intensitäten bezeichnet man als
Depolarisationsgrad ρ :

$$\rho = \frac{I_{\perp}}{I_{\shortparallel}} = \frac{6\gamma^2}{45\bar{\alpha}^2 + 7\gamma^2} \qquad (14)$$

Normalschwingungen, die zu allen Symmetrieelementen
eines Moleküls symmetrisch sind - totalsymmetrische

Schwingungen - können alle Komponenten des Polarisier-
barkeitstensors verändern und damit auch $\bar{\alpha}$ und γ.
Daher ist dann

$$0 \leq \rho \leq 6/7 \tag{15}$$

Bei totalsymmetrischen Schwingungen von Molekülen mit
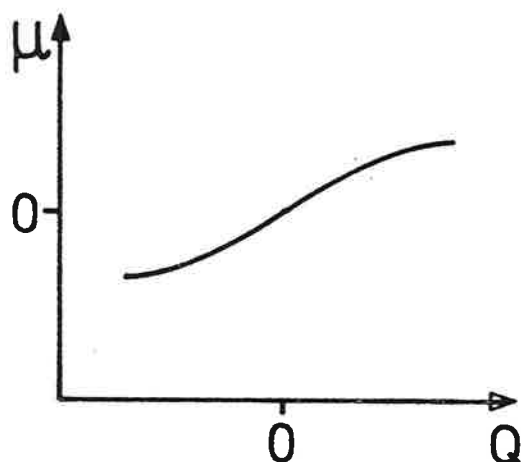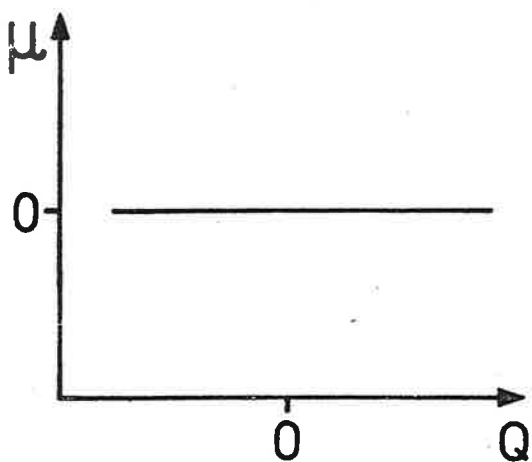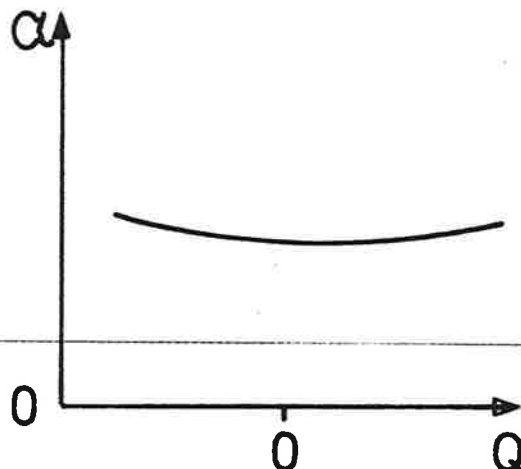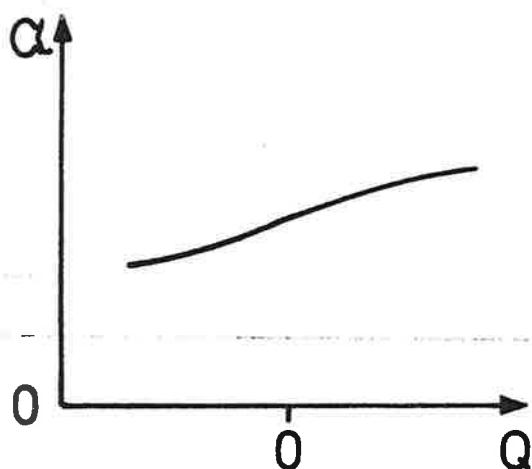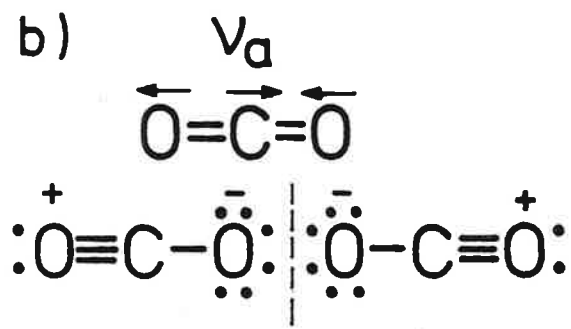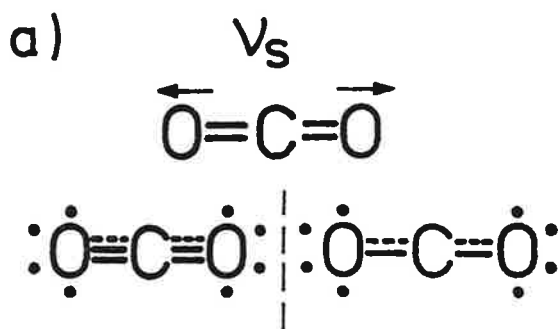kubischer Symmetrie ist dabei $\gamma = 0$, daher:

$$\rho = 0 \tag{16}$$

Bei allen zu irgendwelchen Symmetrieelementen antisymmetrischen
Schwingungen ist $\bar{\alpha} = 0$, damit ist dann

$$\rho = 6/7 \tag{17}$$

Man kann also in den Raman-Spektren von Flüssigkeiten oder
Gasen die totalsymmetrischen Normalschwingungen durch Messung
des Depolarisationsgrades herausfinden!

Das folgende Beispiel soll die Aktivität der Normal-
schwingungen im Raman- und IR-Spektrum anschaulich machen.
Das CO_2-Molekül ist zu zwei Normalschwingungen fähig, bei denen
die Bindungslängen verändert werden, der symmetrischen (ν_s)
und der antisymmetrischen Valenzschwingung (ν_a). Abb. 4 zeigt
schematisch die Veränderungen des Elektronensystems als Folge
dieser Schwingungen. Bei der symmetrischen Valenzschwingung
des CO_2-Moleküls werden beide CO-Bindungen gleichphasig gedehnt
oder gestaucht (Abb. 4 a). Die Coulomb-Anziehung der Valenz-
elektronen durch die Atomkerne wird dabei mit der Frequenz der
Schwingung größer und kleiner. Die Polarisierbarkeit α des
CO_2-Moleküls ändert sich also bei der symmetrischen Valenz-
schwingung; infolgedessen ist diese Schwingung im Ramaneffekt
"aktiv". Bei dieser Schwingung bleibt aber das Dipolmoment des
gesamten Moleküls gleich 0, da die Bindungsdipolmomente beider
Molekülhälften ständig entgegengesetzt bleiben. Nur dann,
wenn sich bei einer Normalschwingung das Dipolmoment des Moleküls
ändert, kann diese durch IR-Strahlung angeregt werden. Diese
Schwingung ist somit im IR-Spektrum "inaktiv".

a) ν_s

$$\overleftarrow{O}=C=\overrightarrow{O}$$

$$:\ddot{O}\!\!\equiv\!\!C\!\!\equiv\!\!\ddot{O}: \;|\; :\ddot{O}\!\!=\!\!C\!\!=\!\!\ddot{O}:$$

b) ν_a

$$\overleftarrow{O}=\overrightarrow{C}=\overleftarrow{O}$$

$$:\overset{+}{O}\!\!\equiv\!\!C\!\!-\!\!\overset{-}{\ddot{O}}: \;|\; :\overset{-}{\ddot{O}}\!\!-\!\!C\!\!\equiv\!\!\overset{+}{O}:$$

Abb. 4: Änderung der Polarisierbarkeit α und des Dipol-
momentes μ bei a) der symmetrischen und b) der
antisymmetrischen Valenzschwingung des CO_2-Moleküls.

Bei der antisymmetrischen Valenzschwingung des CO_2-Moleküls
ist dies alles genau umgekehrt:
Die Polarisierbarkeit des Moleküls in beiden in Abb. 4b
aufgezeichneten Zuständen des Moleküls ist gleich groß. Für
die Gleichgewichtslage Q = O ist $\left(\frac{\partial \alpha}{\partial Q_i}\right)_o = 0$. Das bedeutet: Diese
Schwingung ist nicht ramanaktiv. Die Bindungsdipolmomente
beider CO-Bindungen sind nicht mehr entgegengesetzt gleich
groß. Das gesamte Molekül zeigt also ein Dipolmoment,
dessen Richtung sich im Takt der Schwingung ändert. Die
antisymmetrische Valenzschwingung des CO_2-Moleküls ist
daher IR-aktiv.

Das CO_2-Molekül ist ein einfaches Beispiel für eine
wichtige Auswahlregel, das sog. Alternativverbot: Besitzt
ein Molekül ein Symmetriezentrum, so sind alle zu diesem
Zentrum symmetrischen Schwingungen im IR-Spektrum verboten;
alle dazu antisymmetrischen Schwingungen sind im Raman-
Spektrum verboten. "Verboten" heißt: Diese mechanischen
Schwingungen sind nicht durch Banden im Raman- bzw.
IR-Spektrum zu erkennen.

Die möglichen Schwingungen der Moleküle lassen sich
bezüglich ihrer Symmetrie oder Antisymmetrie zu den Symmetrie-
elementen des Moleküls in "Rassen" einteilen. Welche dieser
"Rassen" IR- oder Raman-aktiv sind, kann man sog. "Charakterta-
bellen" entnehmen, die mit Hilfe der Gruppentheorie
zusammengestellt werden. Durch Abzählung der Anzahl der nur in
jeweils einem der beiden Spektren auftretenden Schwingungen
und derjenigen, die in beiden Spektren vorkommen, kann man
vielfach die Symmetrieeigenschaften eines Moleküls ermitteln.
Dies wird noch erleichtert, wenn man den Depolarisationsgrad
der Raman-Linien mißt, wodurch totalsymmetrische Schwingungen
sofort erkannt werden können.

C.Chemische Bindung und Molekülschwingungen   (nach Ref. 7)

Die Schwingungsspektroskopie der Moleküle (Raman- und
Infrarotspektroskopie) beruht auf den fundamentalen Tatsachen,
daß jedes Molekül oder Molekülion ein ihm eigentümliches
Schwingungsspektrum hat und daß dieses in enger Beziehung
zur Struktur des Moleküls, im weitesten Sinne des Wortes
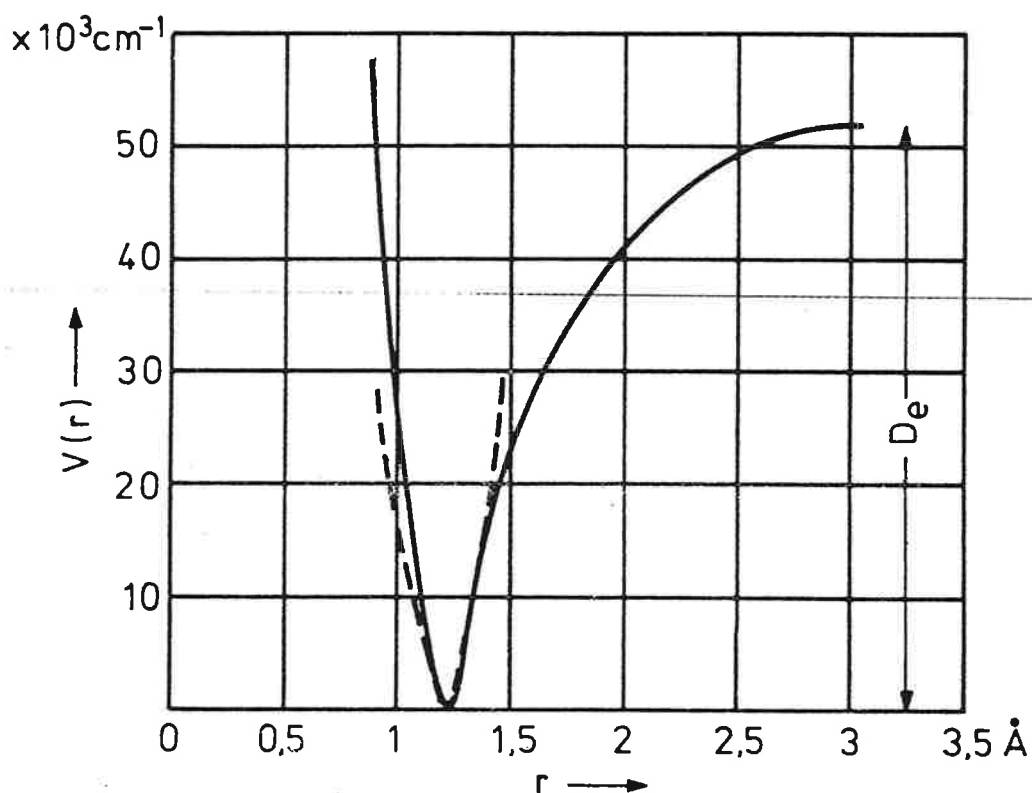(und damit auch zur chemischen Bindung) steht.

Abb. 5: Potentialfunktion eines zweiatomigen Moleküls (O_2)

Um zu einer Vorstellung von Molekülschwingungen zu
kommen, betrachten wir zunächst den einfachsten Fall des
zweiatomigen Moleküls. Dessen Energie ist eine Funktion des
Kernabstandes, wenn von Änderungen der Elektronenenergie
abgesehen wird. Abbildung 5 zeigt die Änderung der potentiellen
Energie der Schwingung der beiden Atome gegeneinander als
Funktion ihres Kernabstandes r . In der Gleichgewichtslage
des Moleküls befindet man sich im Minimum der Potential-

kurve; der zugehörige Gleichgewichtsabstand ist r_e . Für
unsere Betrachtung ist zunächst nur die nähere Umgebung
von Interesse. Bei Verzerrung des Systems, d.h. Änderung
von r gegenüber r_e, tritt eine rücktreibende Kraft auf, bei
Vergrößerung von r eine Anziehung, bei Verkleinerung eine
Abstoßung. Diese Kraft können wir in erster Näherung als
proportional zur Entfernung aus der Ruhelage ansetzen:

$$K = f \cdot (r - r_e) = f \cdot \Delta r.$$

Die Proportionalitätskonstante f heißt Kraftkonstante.
Sie gibt die Stärke der Bindung wieder. Die zugehörige
potentielle Energie ist

$$V(r) = \int f \, \Delta r \, d(\Delta r) = \frac{1}{2} f (\Delta r)^2$$

Wir haben also die Potentialfunktion in der Nähe der
Gleichgewichtslage durch eine Parabel angenähert. Diese
Näherung ist in den meisten Fällen hinreichend.

Die Frequenz einer solchen harmonischen Schwingung
berechnet sich bekanntlich nach

$$\nu = \frac{1}{2\pi} \sqrt{f/\mu}$$

mit $\quad \mu = \dfrac{m_1 m_2}{m_1 + m_2} \quad$ ("reduzierte Masse"); m_i = Masse des
i-ten Atoms

Durch Messung der Schwingungsfrequenzen im Infrarot- oder
im Ramanspektrum lassen sich somit die zugehörigen Kraft-
konstanten einer bestimmten Bindung berechnen, wenn die
reduzierte Masse bekannt ist. Statt der Frequenz ν
(in s^{-1}) wählt man in der Ramanspektroskopie die
Wellenzahl $\tilde{\nu}$ (in cm^{-1}), da diese direkt gemessen
werden kann.
Zusammenhang: $\quad \tilde{\nu} = \frac{1}{\lambda} = \frac{\nu}{c}$.

Beispiele einiger im Schwingungsspektrum experimentell
beobachteter Wellenzahlen (in cm^{-1}), von zweiatomigen
Molekülen (bzw. Radikalen) geordnet nach Bindungstyp:

Typ H-X		Typ X≡Y		Typ X=Y		Typ X-Y	
HCl	2989	CN	2068	OO	1580	FF	892
CH	2824	CO	2168	CC	1642		
OH	3728	NN	2360				

Das Experiment erlaubt uns somit, die Schwingung des
Moleküls längs einer Bindung ("Valenzschwingung") in
nullter Näherung folgendermaßen zu klassifizieren:

Bindungstyp	Wellenzahl, cm^{-1}	Bereich, cm^{-1}
H - X	3000	2600-3700
X≡Y	2200	2000-2400
X=Y	1600	1500-1800
X-Y	1000	800-1200

Beobachtet man in den Raman- bzw. IR-Spektren einer unbe-
kannten Substanz Linien in den angegebenen Bereichen, so
lassen sich daraus sofort Rückschlüsse ziehen, ob bestimmte
Bindungstypen vorhanden sind oder nicht. Man kann sich eine
umfassende Tabelle von sog. charakteristischen Frequenzen
aufstellen und so durch Vergleich mit den beobachteten
Linien in den Spektren direkt die Bindungstypen heraus-
finden.

Abb. 6 zeigt die Wellenzahlbereiche einiger charakteristischer
Frequenzen.

Abb. 7 zeigt als Anwendungsbeispiel ein Ramanspektrum
von Vinylchlorid CH_2_CHCl, in welchem Ramanlinien
bei ca. $3000\ cm^{-1}$, $1600\ cm^{-1}$ und $680\ cm^{-1}$ auf das
Vorhandensein der entsprechenden Bindungstypen C-H, C=C und
C-Cl hinweisen. Die mit δ gekennzeichneten Linien ent-
sprechen sog. Deformationsschwingungen. Bei diesen erfolgt
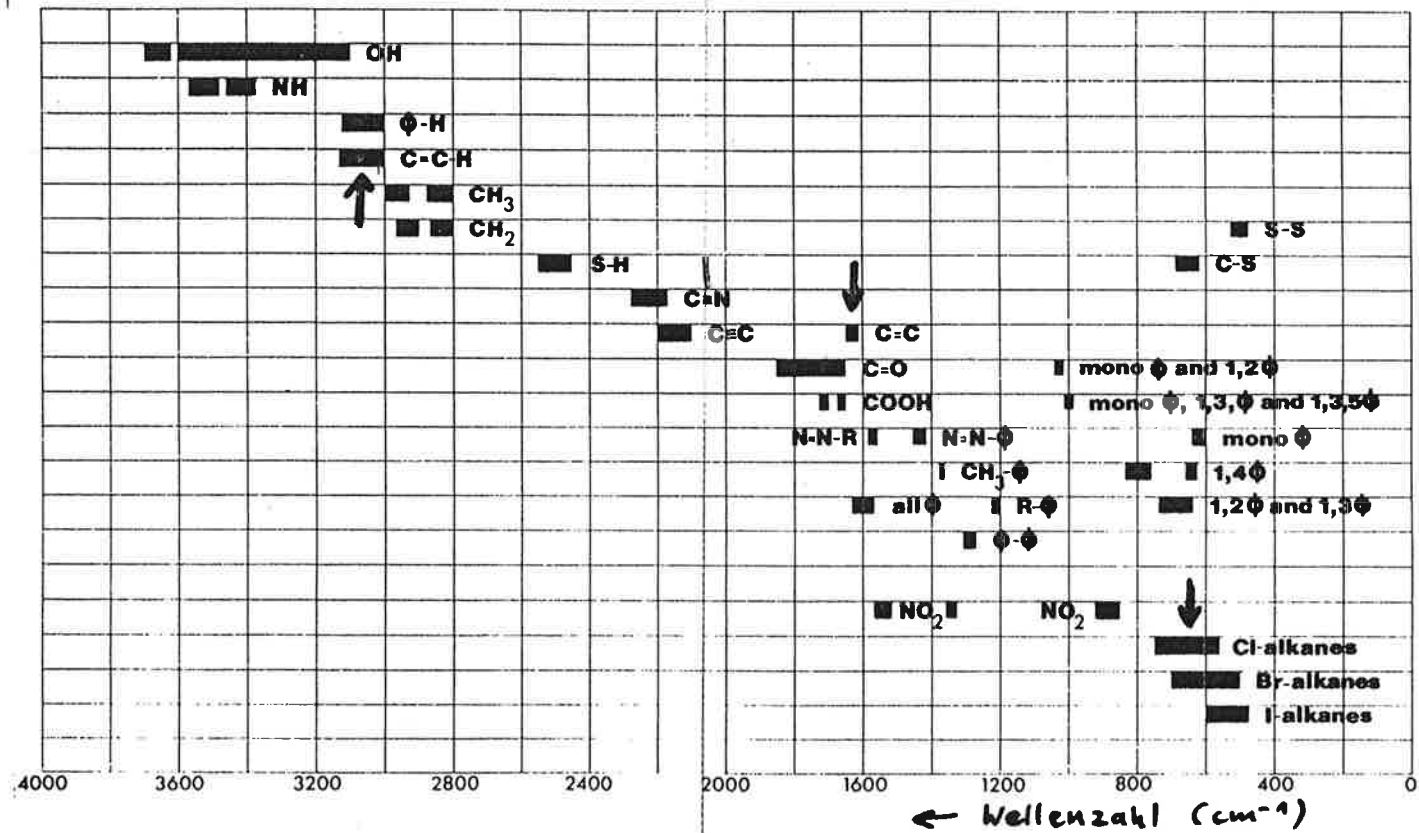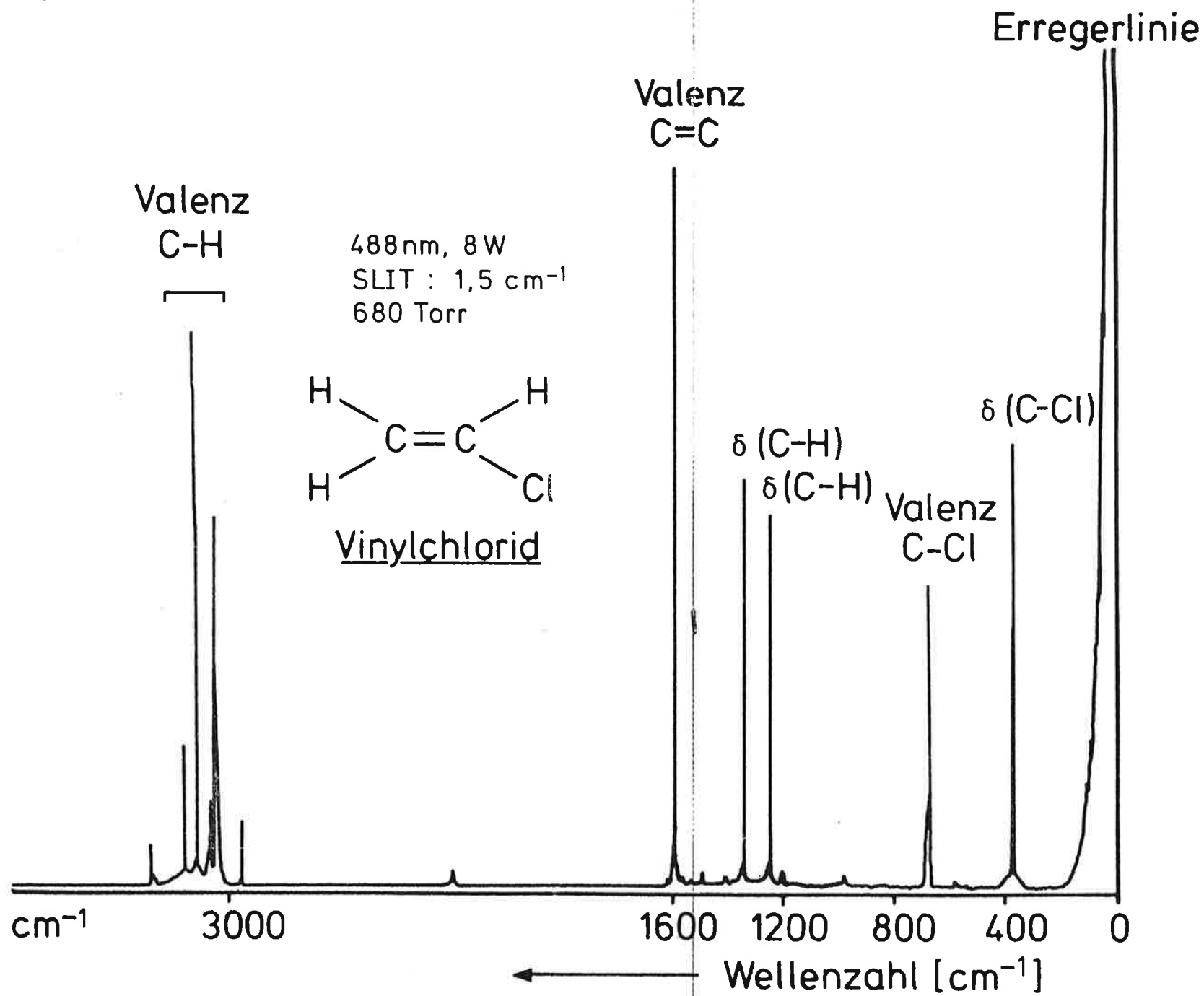vorwiegend eine Änderung der Bindungswinkel.

Abb. 6: Wellenzahlbereiche einiger "charakteristischer Frequenzen"

Erregerlinie

Valenz C=C

Valenz C-H

488 nm, 8 W
SLIT : 1,5 cm⁻¹
680 Torr

H   H
 \   /
  C ═══ C
 /   \
H   Cl

Vinylchlorid

δ (C-H)
δ (C-H)

δ (C-Cl)

Valenz
C-Cl

cm⁻¹   3000   1600 1200 800   400   0

Wellenzahl [cm⁻¹]

Abb. 7: Ramanspektrum von Vinylchlorid im Gaszustand

D. Raman-Spektrometer mit Laser-Lichtquellen

Die wesentlichen Teile einer Raman-Apparatur sind:

Monochromatische Lichtquelle

Dispergierendes Element (meist Doppelmonochromator)

Detektor mit Nachweiselektronik

Abb. 8 zeigt den prinzipiellen Aufbau eines Raman-
Spektrometers.

Es bedeuten:

PR   Polarisations-Rotator; dient zur Bestimmung des
     Depolarisationsgrades der Ramanstrahlung.

L_i Linsen

M   Spiegel

PM   Photomultiplier

PA   Vorverstärker

CR   Photonenzählsystem

MA   Vielkanalanalysator

REC Schreiber

COMP Computer

TT   Teletype

Abb. 9 zeigt die Wellenlängen der für die Raman-Spektroskopie
geeigneter Laser und den Bereich des von ihnen angeregten
Stokes-Raman-Spektrums. Da die Intensität der Raman-Linien
angenähert mit der 4.Potenz der Frequenz der Erregerlinie
ansteigt (y^4-Gesetz) empfiehlt es sich, Erregerstrahlung
möglichst hoher Frequenz, also kleiner Wellenlänge anzuwenden,
zum Beispiel die sehr starken Linien des Argon-Ionen-Lasers
im blauen und grünen Bereich des Spektrums (488 und 515 nm).
Bei farbigen Stoffen, die in diesem Bereich Absorptionsbanden
zeigen, kann meist ohne spezielle Probenanordnungen kein
Raman-Spektrum beobachtet werden. Die Erregerstrahlung wird
dann von der Probe absorbiert: infolgedessen heizt diese
sich auf, verdampft oder zersetzt sich.
Man kann dann eine Erregerlinie aus einem Spektralgebiet
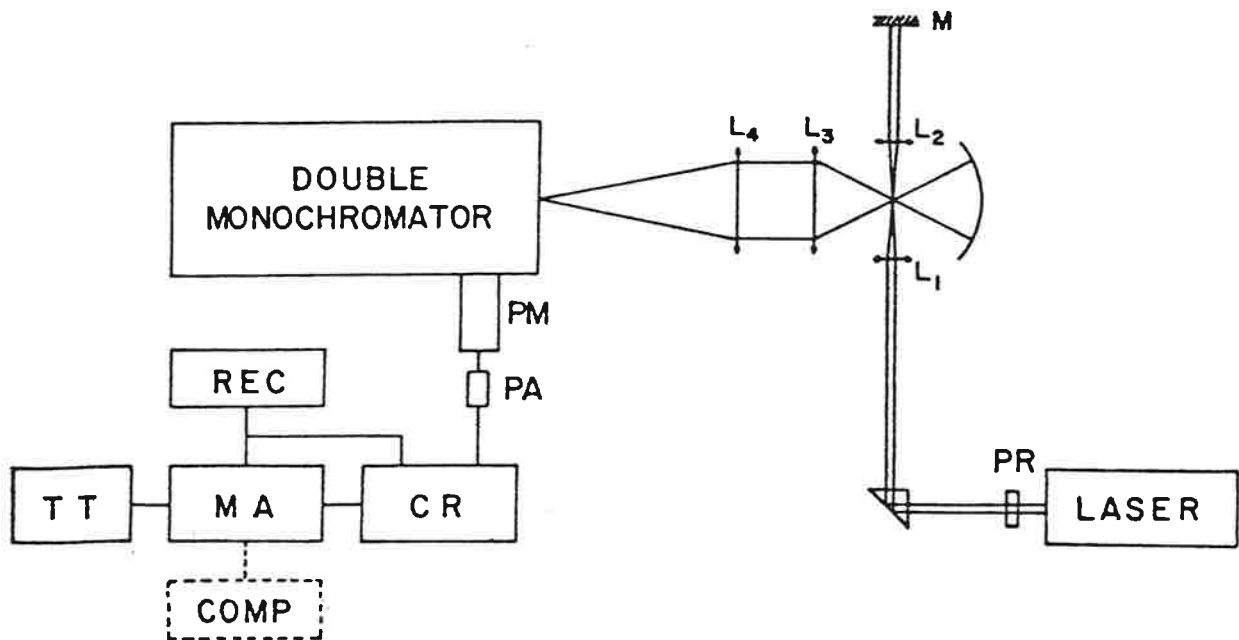anwenden, in dem die Probe nicht absorbiert, z.B. im Roten.

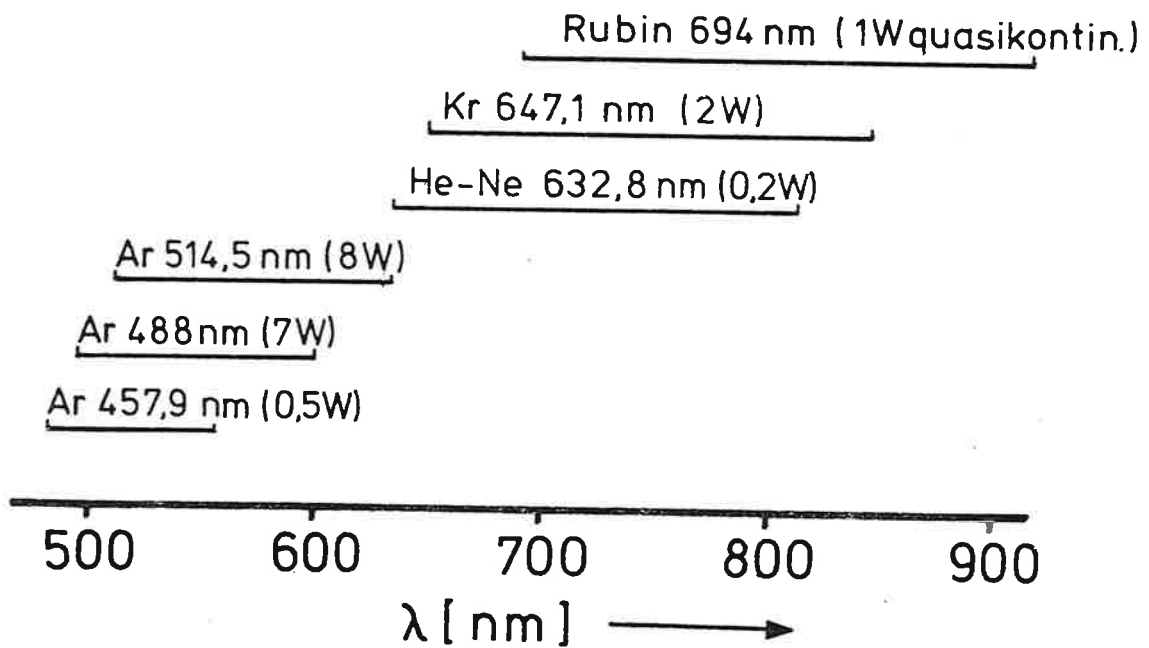**Abb. 8**: Schema einer Laser-Raman-Apparatur. Erklärung siehe Text.

Abb. 9: Verschiedene für die Ramanspektroskopie eingesetzte Laser mit zugehörigen Wellenlängen. Es ist ferner die spektrale Lage des jeweils erregten Ramanspektrums eingezeichnet (Bereich 0 - 3700 cm-1).

Auch mögliche Störungen des Raman-Spektrums durch
Fluoreszenz-Spektren von Verunreinigungen werden bei
längerwelliger Erregerstrahlung verringert.
Jedoch ist die Anwendung von Laser-Lichtquellen aus dem
roten Bereich des Spektrums wegen des ν^4-Gesetzes nicht
allgemein ratsam, außerdem sind die Strahlungsempfänger
(meist Photomultiplier) für diesen Spektralbereich weniger
empfindlich als für den blau-grünen Bereich des Spektrums.

Am günstigsten ist es, wenn man den Laser-Strahl
fokussiert und die Probe in den Bereich des Fokus stellt.
Dadurch erreicht man bei einer kleinen Probe eine große
Bestrahlungsdichte. Je nach der Brennweite der fokussierenden
Linse (L_1, Abb. 8) hat der Strahl im Fokus einen Durchmesser
von 10-100 μm. Mit einer vergrößernden lichtstarken Optik
(L_3, L_4) bildet man den vom Laser beleuchteten fadenförmigen
Bereich der Probe in den Eintrittsspalt eines Monochromators
ab. Die bei dieser Probenanordnung erforderliche Probenmenge
ist durch das Volumen eines Röhrchens gegeben, das den
Laser-Strahl im Bereich des Fokus umschließt und eine Länge
von ca. 2-5 mm besitzt, so daß der Eintrittsspalt bei
vergrößernder Abbildung voll ausgeleuchtet wird. Die
Kombination L_2, M sowie ein Hohlspiegel erhöhen den
genutzten Strahlungsfluß von Erreger- und Raman-Strahlung.

Die Proben liefern meist noch gleichzeitig mit der
Raman-Strahlung um drei bis acht (bei Kristallpulvern sogar
bis zu zehn) Zehnerpotenzen stärkere "unverschobene"
Erregerstrahlung in das Ramanspektrometer, die sich als
störender Untergrund bemerkbar macht. Ein guter Monochromator
schwächt das Falschlicht um etwa fünf Zehnerpotenzen.
Man muß daher zwei oder sogar drei hintereinanderschalten,
wobei oft nur einer die spektrale Zerlegung leistet, die
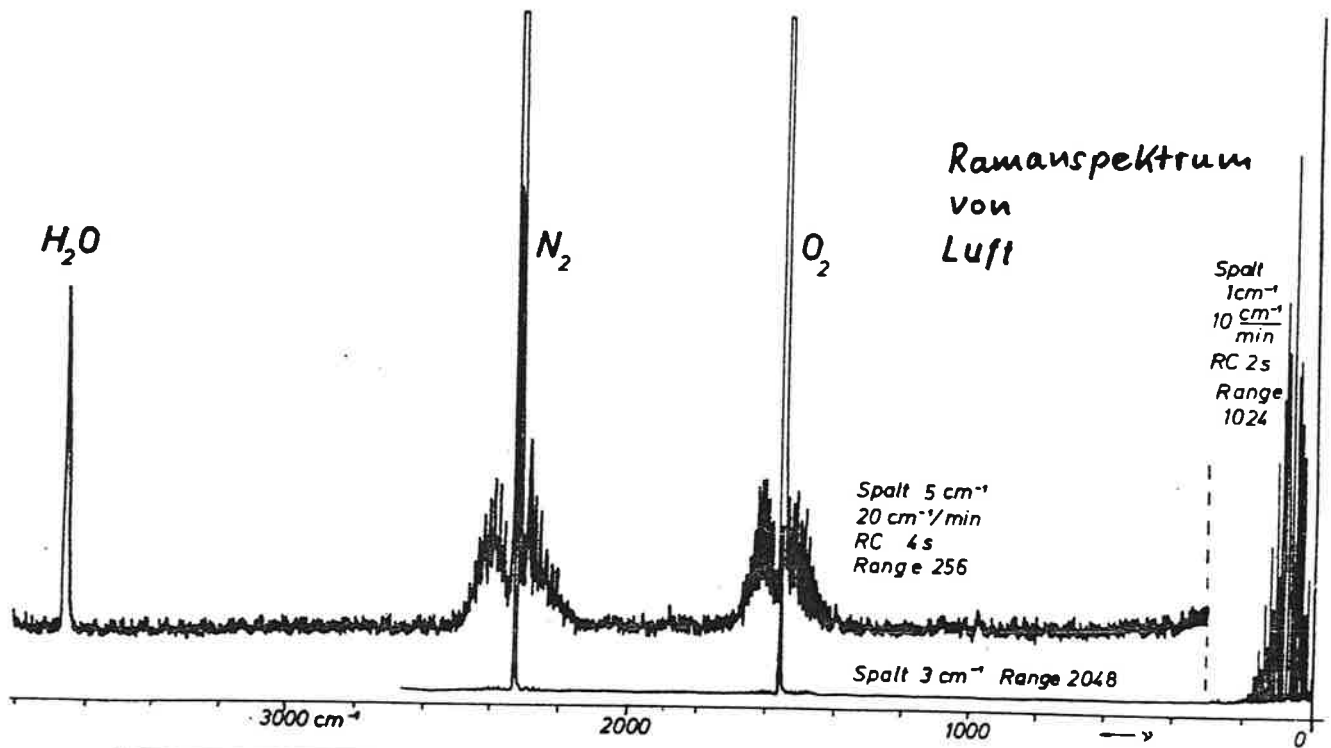beiden anderen aber - reichlich kostspielige - Filter sind.

Das spektral zerlegte Licht wird mit einem Photo-
multiplier in ein elektrisches Signal umgewandelt.
Die von den auf die Photokathode auffallenden Photonen
ausgelösten Elektronen liefern an der Anode des PM jeweils
einen Stromimpuls, der, verstärkt über einen Vorverstärker,
mit einem Photonenzählsystem als Einzelimpuls gezählt
werden kann. Die Zahl der pro sec registrierten Impulse
ist somit ein Maß für die Intensität der auffallenden Raman-
strahlung. Durch kontinuierliches Drehen des Gitters im
Monochromator wandern die Ramanlinien am Austrittsspalt
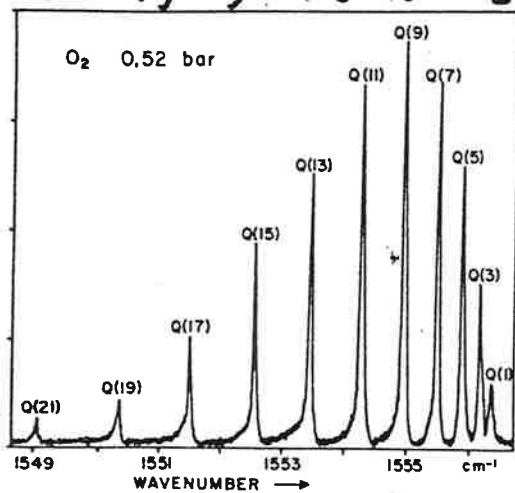des Monochromators vorbei.
Mißt man gleichzeitig mit einem an den Photonenzähler
angeschlossenen Schreiber die Intensität als Funktion der
Zeit, so kann ein Ramanspektrum direkt photoelektrisch
registriert werden. Das Spektrum kann aber auch digital
in einem Vielkanalanalysator abgespeichert und später
mit einem Computer weiterverarbeitet werden.

E. Beispiele von Ramanspektren

Die nachfolgend gezeigten Ramanspektren wurden mit
Laser-Raman-Apparaturen direkt photoelektrisch registriert.
Die kleine Auswahl zeigt, daß die Raman-Spektroskopie - über
die klassischen Gebiete Physik und Chemie hinaus - inzwischen
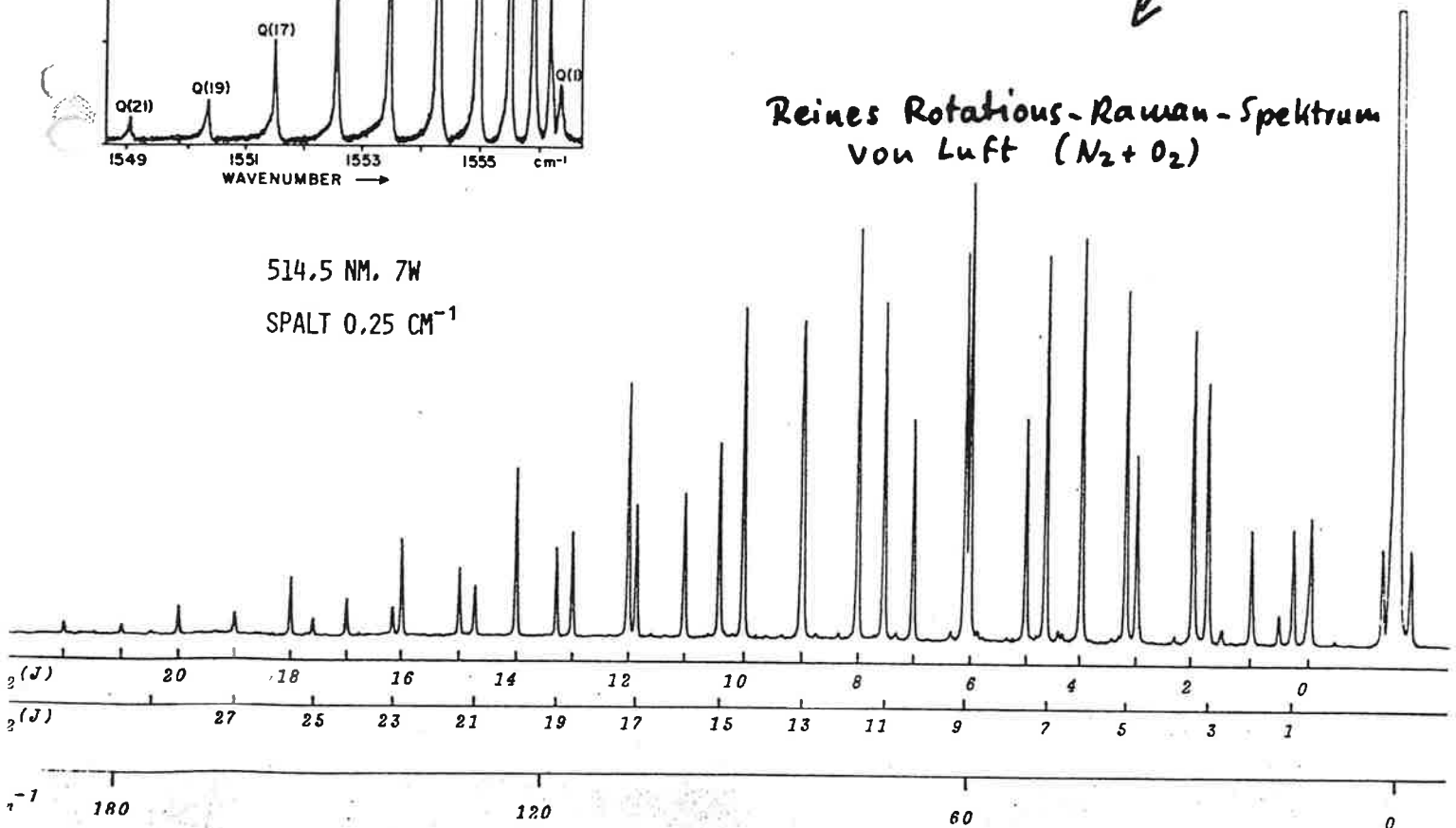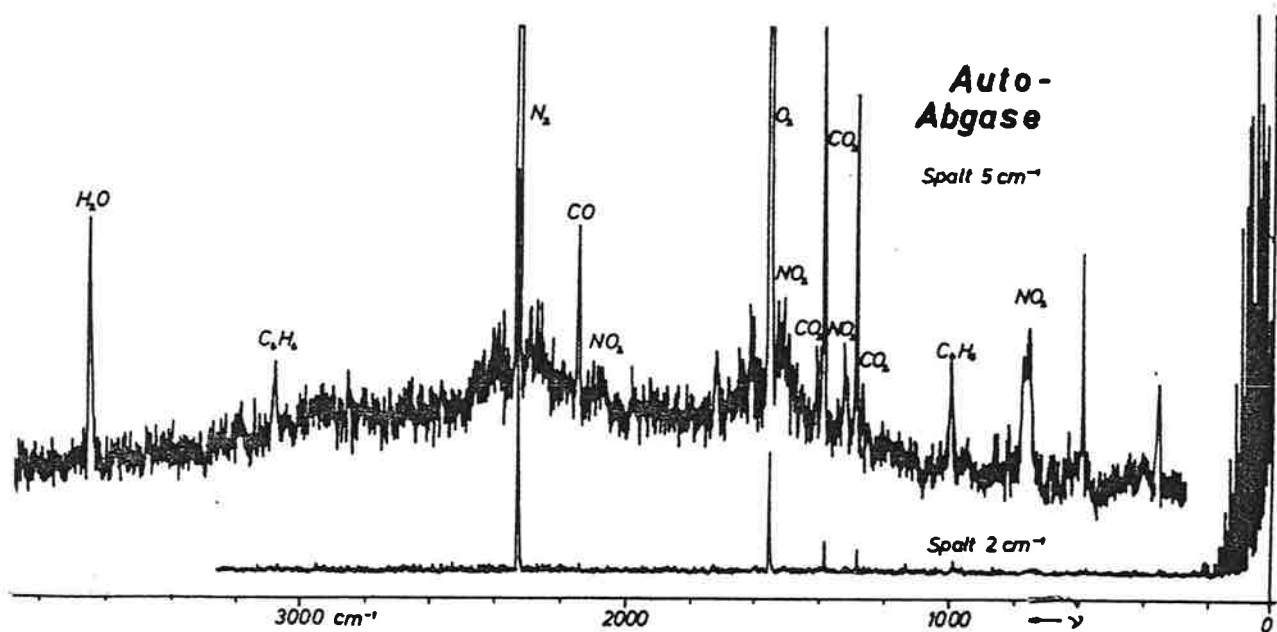auch in den Bereichen Biologie und Medizin eingesetzt wird.

H_2O

N_2

O_2

Ramanspektrum
von
Luft

Spalt
1 cm⁻¹
10 $\frac{cm^{-1}}{min}$
RC 2 s
Range
1024

Spalt 5 cm⁻¹
20 cm⁻¹/min
RC 4 s
Range 256

Spalt 3 cm⁻¹ Range 2048

3000 cm⁻¹

2000

1000

⟶ ν

0

Schwingungslinie von O_2

O_2 0,52 bar

Q(9)
Q(11) Q(7)
Q(13) Q(5)
Q(15)
Q(17) Q(3)
Q(19) Q(1)
Q(21)

1549   1551   1553   1555   cm⁻¹
WAVENUMBER ⟶

514,5 NM. 7W

SPALT 0,25 CM⁻¹

Reines Rotatious-Raman-Spektrum
von Luft ($N_2 + O_2$)

| $O_2(J)$ | | 20 | | 18 | | 16 | | 14 | | 12 | | 10 | | 8 | | 6 | | 4 | | 2 | | 0 |
| $N_2(J)$ | | | 27 | | 25 | | 23 | | 21 | | 19 | | 17 | | 15 | | 13 | | 11 | | 9 | | 7 | | 5 | | 3 | | 1 |

cm⁻¹   180   120   60   0

Ramanspektrum von Auto-Abgasen, Laserleistung ca. 1 W bei 515 nm

Raw Carrot
(β-Carotene)

C=C

C-C

Strukturformel von β-Carotin ($C_{40}H_{56}$)

Abb.: Ramanspektrum einer rohen Karotte

Fig 10 Raman spectra of FB viruses in 0.05 M NaCl at 32°C and pH 9. (Curve a) Pf1: concentration C=108 μg/μl; excitation wavelength (λ)= 488.0 nm; radiant power (P)=100 mW; slit width (Δσ)=5 cm⁻¹; scan rate (r)=50 cm⁻¹/min; rise time (t)=1 sec; amplification (A)=3x. (Curve b) Pf1: Δσ=10 cm⁻¹; t=3 sec; A=1x; other conditions as in (a). (Curve c) fd: C=147 μg/μl; λ=514.5 nm; P= 100 mW; Δσ=5 cm⁻¹; r=50 cm⁻¹/min; t=1 sec; A=3x. (Curve d) fd:Δσ=9 cm⁻¹; t=3 sec; A=1x; other conditions as in (c). (Curve e) Pf1: A=x/3; other conditions as in (b). (Curve f) fd: A=x/3; other conditions as in (d).

Frequencies of prominent lines are in cm⁻¹, and assignments to molecular subgroups are denoted by standard abbreviations. Abbreviations: str, stretching; def, deformation; CH, carbon-hydrogen bond; CC, carbon-carbon bond; CN, carbon-nitrogen bond; A, T, C, and G, adenine, thymine, cytosine, and guanine; ala, alanine; met, methionine; phe, phenylalanine; trp, tryptophan; tyr, tyrosine; Am, amide. This virus contains a small percentage of nucleic acid, and therefore its Raman spectrum is dominated by vibrational frequencies of the coat protein molecules. (From [46].)
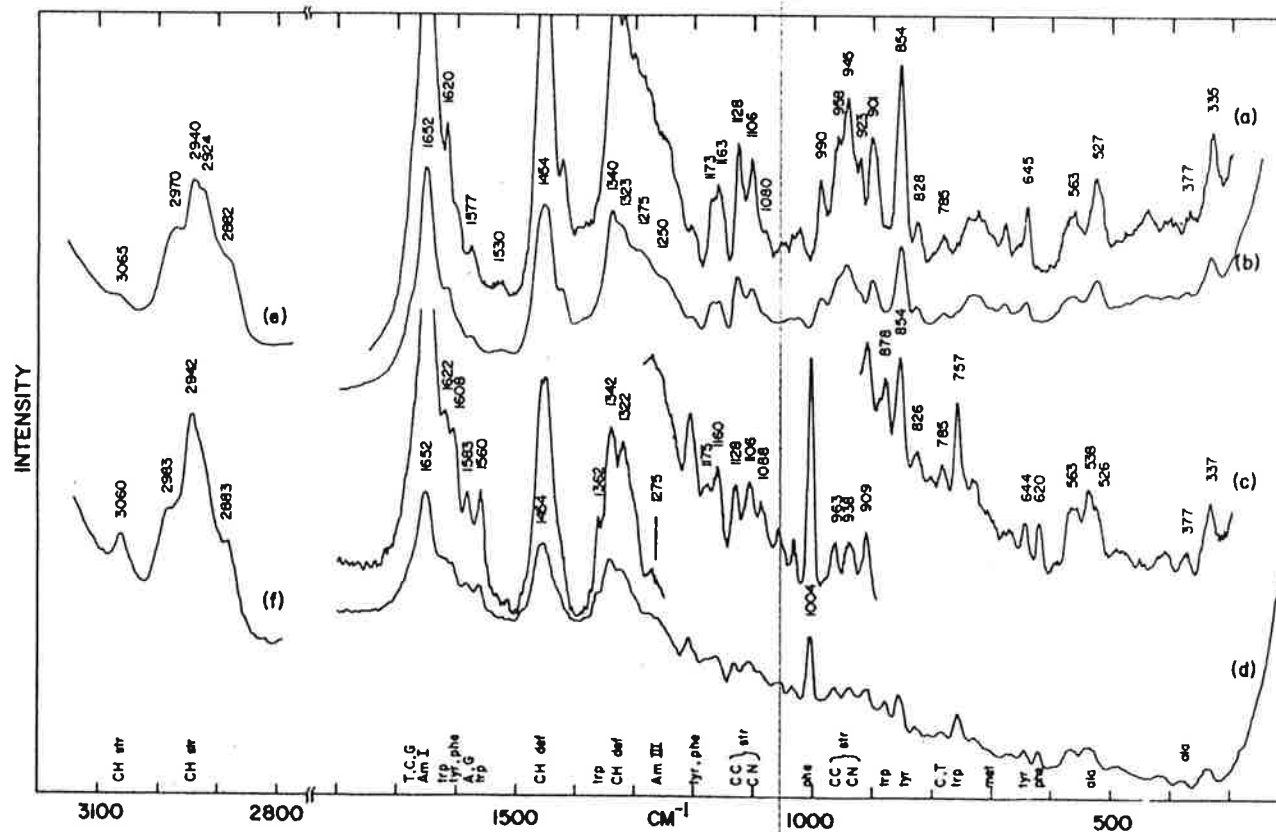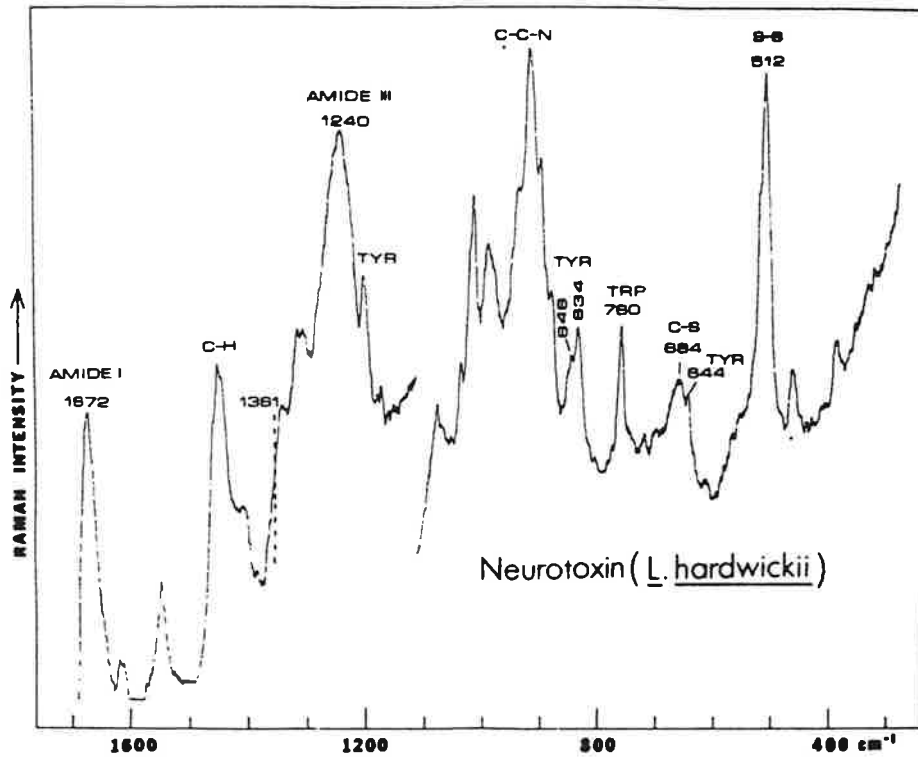

Ramanspektren von Viren

Fig 6   Raman spectrum of purified sea snake neurotoxin. Reproduced from *J. Biol. Chem.*, 250, 1782 (1975) by N.T. Yu, T.S. Lin, and A.T. Tu. Most sea snake toxins show similar Raman spectra as the *Lapemis hardwickii* neurotoxin. The major toxin of *Lapemis hardwickii* (Hardwick's sea snake) is used as an example in this figure. This indicates that most sea-snake-neurotoxins have very similar protein conformation regardless of the species and geographical origins of the sea snakes themselves. The spectrum is loaded with information on protein structure of the toxin. Amide I and III (1672 and 1240 cm⁻¹) bands indicate anti-parallel β structure of the toxin molecule. The lack of 1361 band indicates that the tryptophan group is exposed. The intensity ratio at 846 and 834 cm⁻¹ indicates the tyrosine component is buried inside the fold of the toxin molecule. The disulfide stretching band is clearly shown at 512 cm⁻¹ indicating the conformation of gauche-gauche-gauche.
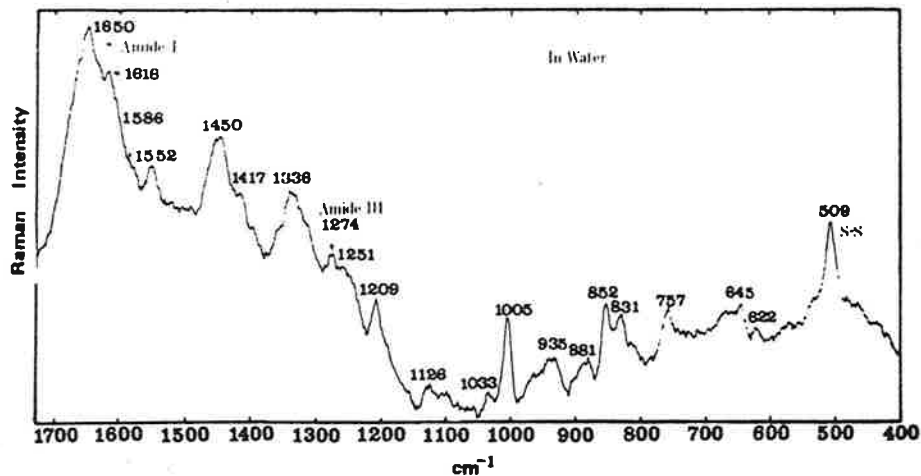

Fig 8   Raman spectrum of Mojave toxin isolated from Mojave rattlesnake venom (Reproduced from *Biochem. Biophys. Res. Comm.*, 68, 1139 (1976) by A.T. Tu, B. Prescott, C.H. Chou, and G.J. Thomas). The Amide I and Amide III region by the 1650 and 1274 cm⁻¹ frequencies, respectively, is a clear indication of a predominantly α-helical backbone conformation. In contrast to Mojave toxin, sea snake neurotoxins predominantly consist of anti parallel β and β-turn structures (Fig. 3, Fig. 6). The appearance of a strong and sharp line at 509 cm⁻¹ is due to four disulfide linkages. The sharp and symmetrical shape of this line indicates a high probability that the geometries of all four disulfide linkages are similar. The intensity ratio of 0.71 for 828:853 cm⁻¹ is indicative of exposed (completely solvated) tyrosol groups. Probably the tyrosine components are located on the surface of the protein molecule.

Ramanspektren von Schlangengiften

    oben : Seeschlange

    unten : Klapperschlange

Zeitaufgelöste
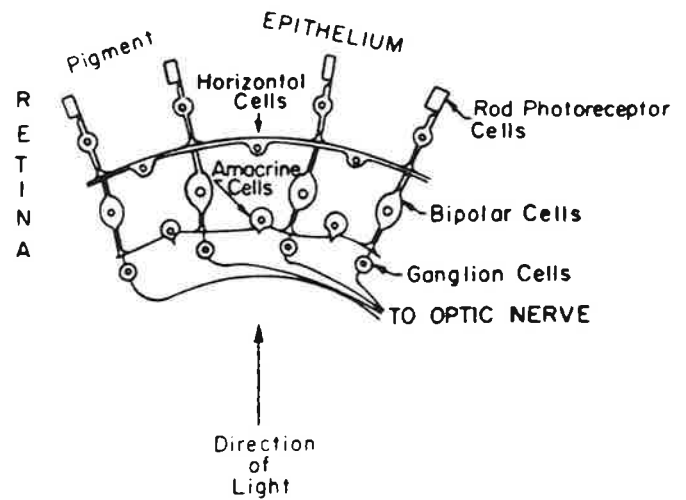Ramanspektroskopie
an Molekülen die
am Sehprozess
teilnehmen

Fig 2 Cross section of the retina. After passing through a neuronal layer (ganglion cells, bipolar cells, amacrine cells, and horizontal cells) light impinges on the rod photoreceptor cells which absorb the light and generate a neuronal response. Light that passes through the retina finally strikes a pigmented layer called the pigment epithelium.

Rhodopsin is
11-CIS retinal + a
membrane glycoprotein
matrix called opsin

498 nm

psec ⟍ hν

Batho Rhodopsin
543 nm

nsec

Lumi Rhodopsin
497 nm

μsec

Meta Rhodopsin I
460 nm

msec

Meta Rhodopsin II
380 nm

minutes

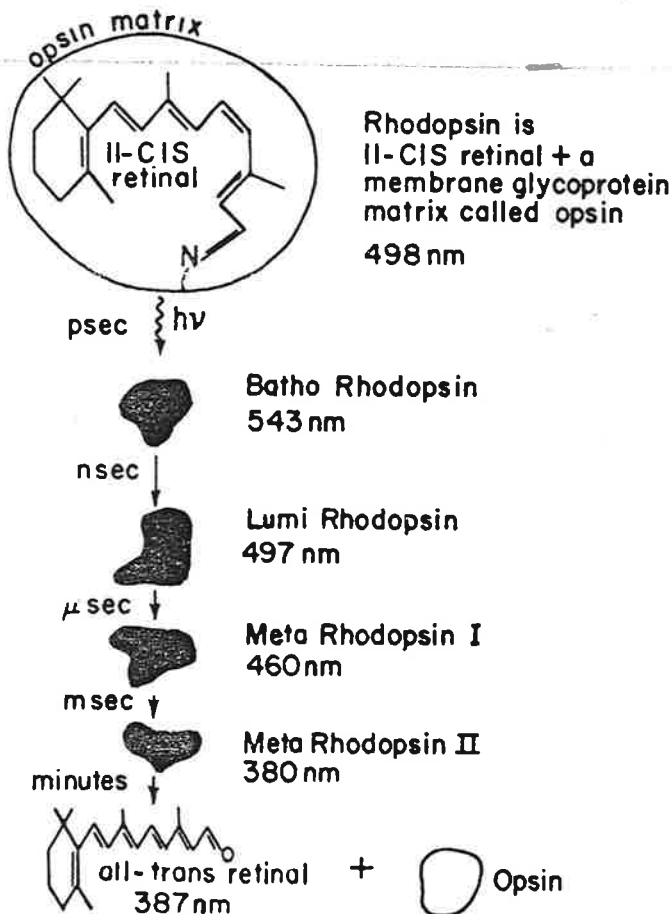all-trans retinal + Opsin
387 nm

Fig 4 The chemical composition and the light-induced conformational changes of rhodopsin, the principal light absorber in the eye. Rhodopsin is a large molecule consisting of a small (45-atom) unit called retinal embedded in a matrix (of sugar, lipid, and protein) called opsin. The center of photochemical activity is the double-bonded (12-atom) segment of the retinal and those atoms electronically coupled to this region of the molecule. It is the vibration of these atoms that is selectively observed in the resonance Raman spectrum of rhodopsin.
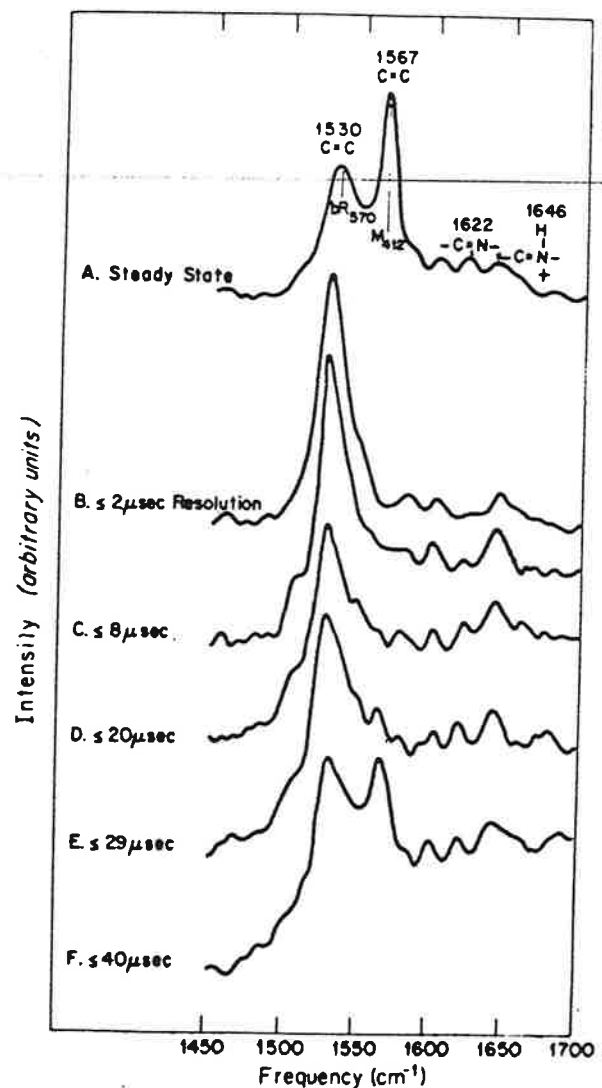

Fig 7 Steady state and kinetic resonance Raman spectra of bacterial rhodopsin over a limited frequency region. These spectra illustrate the dynamics of the deprotonation of the Schiff base linkage as a function of delocalization and relocalization of electron density in the C=C bond.

Tabelle 30. *UR-Spektren von Kettenmolekülen* WXYZ (C_s)

Molekül	Zustand	$\nu_1(A')$ $\nu(WX)$	$\nu_2(A')$ ν	$\nu_3(A')$ ν	$\nu_4(A')$ $\delta(WXY)$	$\nu_5(A')$ $\delta(XYZ)$	$\nu_6(A'')$ τ	Lit.
HN$_3$	gas	3336	2140	1274	1150	522	672	288
DN$_3$	gas	2480	2141	1183	955	498	638	288
FN$_3$	Matrix	869	2034	1086	654	503	—	787
ClN$_3$	Matrix	723	2066	1144	—	520	—	787
BrN$_3$	Matrix	687	2062	1160	—	530	—	787
HNCO	gas	3531	2274	1327	797	572	670	524
HNCS	gas	3539	1980	851	470	542	615	59
DNCS	gas	2644	1944	854	374	483	566	59
HOCN	Matrix	3506	2294	1098	1241	460	(438)	562
DOCN	Matrix	2590	2292	1093	957	437	—	562
ClSCN	Läg	520	2162	678	—	353	—	826
BrSCN	Läg	451	2157	676	—	369	—	826
JSCN	Läg	372	2130	700	—	362	—	826
HOBO	gas	3680	2030	—	1420	650	—	1174
trans-HONO	gas	3590	1700	793	1267	598	545	502
cis-HONO	gas	3425	1639	855	1370	525	638	591
trans-DONO	gas	2658	1695	739	1015	592	416	
cis-DONO	gas	2537	1620	817	1086	517	—	842
cis-HNSO	gas	3345	1261	1090	911	453	759	912
cis-DNSO	gas	2480	1257	1055	757	410	594	912

Das F—N=N—Cl ist wahrscheinlich eben (Typ II oder III). *UR*-Banden wurden bei 1540 = ν(NN), 1060 = ν(NF) und 670 = ν(NCl) beobachtet [882].

f) Weitere vieratomige Moleküle

Im P$_4$ sind die P-Atome in den Ecken eines Tetraeders angeordnet. Die Punktgruppe ist T_d (vgl. Tab. 31). Das *Ra*-Spektrum der flüssigen Substanz ist [109, 1136] 606 = $\nu_1(A_1)$, 363 = $\nu_2(E)$, 465 = $\nu_3(F_2)$. Für die Kraftkonstante f(PP) wird 2,07 mdyn/Å berechnet [875].

Die Moleküle Li$_2$O$_2$ [1170] und Li$_2$F$_2$ [949] wurden schwingungsspektroskopisch in inerter Matrix nachgewiesen. Sie sind ringförmig gebaut:

$$\mathrm{Li} \underset{F}{\overset{F}{\diamondsuit}} \mathrm{Li}$$
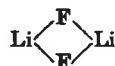
die Symmetrie ist D_{2h} (vgl. Tab. 43, S. 78).

4. Fünfatomige Moleküle

a) XY$_4$, tetraederförmig (T_d)

Das Atom X liegt im Schwerpunkt eines Tetraeders, die Atome Y in den Ecken. Es sind vier dreizählige Achsen vorhanden, welche durch die Bindungen X—Y gehen, ferner drei zweizählige Achsen, welche senkrecht zueinander stehen und die Valenzwinkel halbieren. Diese zweizähligen Achsen sind gleichzeitig vierzählige Drehspiegelachsen. Jede der 6 denkbaren Bruchteile XY$_2$ des Moleküls definiert eine Symmetrieebene; die Schnittlinien von je drei dieser Ebenen sind die dreizähligen Achsen. Die zugehörige Punktgruppe ist T_d (vgl. Tab. 31). Die

Schwingungsformen zeigt Abb. 21; für die entarteten Schwingungen ist nur je eine Komponente angegeben. Die Zuordnung der beobachteten Frequenzen zu den Normalschwingungen ist in Kap. I, S. 24 beschrieben.
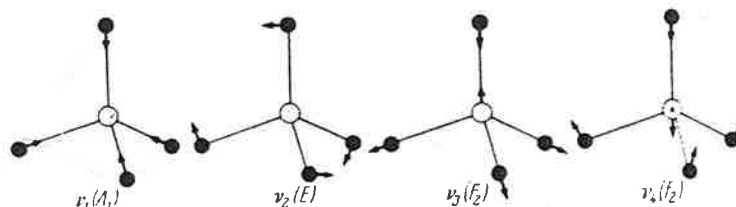

Abb. 21. Schwingungsformen von Tetraedermolekülen XY₄ (T_d)

Die Tetraedermoleküle sind der spektroskopisch am häufigsten untersuchte Molekültyp. Zweckmäßigerweise wird daher eine Unterteilung in drei Gruppen vorgenommen: 1. Hydride, 2. Halogenide, 3. Oxide, Oxo- und Thioionen.

Tabelle 31. *Punktgruppe T_d. Symmetrieelemente:* $4C_3, C_x, C_y, C_z, S_{4x}, S_{4y}, S_{4z}, \sigma_x,$ $\sigma_x, \sigma_z, 3\sigma_v$

Klasse	C_3	S_4	C_2	σ	Ra	UR	Abzählung		
							X₄ Tetraeder	XY₄ Tetraeder	X(YZ)₄ Tetraeder
A_1	s	s	s	s	p	—	1ν	1ν	2ν
A_2	s	as	s	as	—	—	—	—	2δ
E	e	e	s	e	dp	—	1δ	1δ	1δ
F_1	e	e	e	·e	—	—	—	—	
F_2	e	e	e	e	dp	$\mathfrak{M}$	1ν	1ν, 1δ	2ν, 2δ

1. Hydride. Im *Ra*-Spektrum ist ν_1 stets sehr intensiv (bei CH₄ auch ν_3), ν_2 und ν_4 sind schwächer als ν_1, ν_3 ist meist sehr schwach. Im *UR* wird bei gasförmigen Substanzen erwartungsgemäß ν_1 nicht gefunden, was als Beweis für streng kubische Symmetrie gewertet werden kann. Dagegen tritt ν_2 im *UR* von gasförmigen CH₄, CD₄, SiH₄, GeH₄ und GeD₄ — wenn auch sehr schwach — auf. Dies bedeutet keine Unsymmetrie, sondern ist auf eine Coriolis-Wechselwirkung zwischen ν_4 und ν_2 zurückzuführen. Die Veränderungen der Spektren beim Übergang vom gasförmigen zum flüssigen, festen oder gelösten Zustand sind sehr gering. Die Frequenzen verschieben sich um höchstens 1% nach kleineren Wellenzahlen.

Bei den Hydrid-Ionen ist in Lösung die Tetraedersymmetrie gewahrt (BH₄⁻ und AlH₄⁻). Im festen Zustand bedingt die Gitterstruktur meist eine Unsymmetrie, so daß Aufspaltungen der Frequenzen beobachtet wird. Diese Aufspaltungen sind im allgemeinen nicht groß, so daß man der Einfachheit halber die beobachteten Schwingungen so zuordnet, als ob Tetraedersymmetrie vorläge, so z. B. bei PH₄⁺ und AsH₄⁺. Die Ammoniumsalze sind eingehend untersucht worden. Tetraedersymmetrie des NH₄⁺-Ions wurde beim NH₄Cl, NH₄Br, (NH₄)₂SnCl₆ und (NH₄)₂SiF₆ gefunden, in allen übrigen untersuchten Fällen geringere Symmetrien. Die

Weitere hierhergehörige Substanzen sind GeO_4^{4-} (im Spinelltyp mit unverzerrten Tetraedern $\nu_3 \approx 690$, $\nu_4 \approx 430$ [1101]), XeO_4 (UR gas $\nu_3 = 877$, $\nu_4 = 306$ [972]), TiO_4^{4-} (Ba_2TiO_4 $\nu_1 = 745$ [126], $\nu_3 \approx 720$ [1100]), CrO_4^{3-} ($\nu_3 = 880$) und CrO_4^{4-} ($\nu_3 = 770$) [1233], MnO_4^{2-} ($\nu_3 = 850$) und MnO_4^{3-} ($\nu_3 = 770$) [922], RuO_4^{-} ($\nu_3 \approx 835$ [1192]).

Die Frequenzgleichungen lauten hier:

$$\lambda_1 = (f + 3f')\mu_y$$

$$\lambda_2 = (d - 2d' + d'')3\mu_y$$

$$\lambda_3 + \lambda_4 = (f - f')\left(\frac{4}{3}\mu_x + \mu_y\right) + 2(d - d'')\left(\frac{8}{3}\mu_x + \mu_y\right) - \frac{16}{3}\sqrt{2}(g' - g'')\mu_x$$

$$\lambda_3 \cdot \lambda_4 = [(f - f')(d - d'') - 2(g' - g'')^2]2\mu_y(4\mu_x + \mu_y).$$

Zur Berechnung der Kraftkonstanten sind Isotopenfrequenzen, Coriolis-Kopplungskonstanten, Schwingungsamplituden und Raman-Intensitäten herangezogen worden. Einige so erhaltene Ergebnisse zeigt Tab. 35. Die Methode von Fadini (vgl. S. 33) liefert hier gute Näherungswerte. In den Tab. 32, 33 und 34 sind die wichtigsten Konstanten f und d mit aufgeführt, die hiernach erhalten wurden [997].

Als einfache Näherung kann man noch willkürlich $(g' - g'') = 0$ setzen. Dies ergibt für die anderen Konstanten bei den Hydriden gute Werte. Für die übrigen Moleküle erhält man nur dann brauchbare Zahlen, wenn das Zentralatom X schwerer als die Außenatome Y ist, da dann der Einfluß von $(g' - g'')$ weniger ins Gewicht fällt.

Tabelle 35. *Kraftkonstanten einiger Tetraedermoleküle*

Molekül	Methode	f	f'	$d-d''$	$d'-d''$	$g'-g''$	Lit.
CH_4	Coriolis	4,95	0,03	0,42	− 0,02	0,14	297
	$(g' - g'') = 0$	4,90	0,05	0,42	− 0,02	[0]	
CF_4	Isotopen	6,27	0,99	1,12	0,21	0,45	450
	Coriolis	6,97	0,75	1,01	0,15	0,59	297
	Fadini	6,93	0,77	1,02	0,16	0,57	997
SiF_4	Isotopen	6,57	0,21	0,44	0,09	0,19	517
	Coriolis	6,16	0,33	0,47	0,10	0,03	297
	Fadini	6,33	0,28	0,45	0,09	0,09	997
	$(g' - g'') = 0$	6,11	0,36	0,47	0,10	[0]	
BF_4^-	Isotopen	5,19	0,51	0,69	0,11	0,51	996
	Fadini	4,87	0,62	0,72	0,13	0,43	997
CCl_4	Amplituden	3,59	0,24	0,38	0,03	0,36	800
	Ra-Int.	3,12	0,42	0,44	0,05	0,29	177
	Fadini	3,25	0,37	0,42	0,05	0,31	997
$SiCl_4$	Amplituden	2,97	0,26	0,26	0,05	0,05	1284
	Fadini	3,03	0,23	0,23	0,04	0,09	997
	$(g' - g'') = 0$	2,79	0,30	0,27	0,06	[0]	

b) ZXY_3, tetraederförmig (C_{3v})

Diese Moleküle leiten sich von den vollsymmetrischen Tetraedern XY_4 ab, worin ein Atom Y durch ein Atom Z substituiert ist. Es ist dann nur noch eine dreizählige Achse vorhanden sowie drei dazu senkrechte Symmetrieebenen (Punktgruppe C_{3v}, vgl. Tab. 22, S. 56). Die Schwin-

gungsformen sind in Abb. 22 dargestellt, für die entarteten Schwingungen ist wieder nur eine Komponente angegeben. Die symmetrische Deformationsschwingung der Klasse A_1 verändert sowohl die Winkel YXY als auch ZXY; dagegen werden bei der entarteten Deformationsschwingung ν_5 im wesentlichen nur die Winkel YXY verändert, bei ν_6 die Winkel ZXY. Die letztere wird häufig als „rocking"-Schwingung bezeichnet.

Tab. 36 enthält die Spektren einer Reihe hierhergehöriger Substanzen. Die Zuordnung zu den Klassen ist meist gesichert und stützt sich auf

Tabelle 36. *Frequenzen von tetraederförmigen Molekülen* ZXY_3 (C_{3v})

Molekül	Methode Zustand	$\nu_1(A_1)$ $\nu(ZX)$	$\nu_2(A_1)$ $\nu_s(XY)$	$\nu_3(A_1)$ δ_s	$\nu_4(E)$ $\nu_a(XY)$	$\nu_5(E)$ $\delta_a(XY_2)$	$\nu_6(E)$ $\delta_a(ZXY)$	Lit.
CH_3F	UR gas	1049	2965	1464	3006	1467	1182	1030
CH_3Cl	Ra, UR gas	732	2967	1355	3042	1455	1015	279, 1165, 1285
CH_3Br	Ra, UR gas	610	2972	1306	3060	1449	954	279, 1165, 1285
CH_3J	UR gas	533	2970	1251	3062	1439	881	279, 1285
SiH_3F	UR gas	872	2206	990	2196	943	728	820, 1222
SiH_3Cl	UR gas	551	2201	949	2195	954	664	820, 1222
SiH_3Br	UR gas	430	2200	930	2196	950	633	747, 820, 1222
SiH_3J	UR gas	362	2192	903	2206	941	592	280, 680, 1222
GeH_3F	UR gas	689	2121	859	2132	874	643	369
GeH_3Cl	UR gas	422	2120	848	2129	874	602	369
GeH_3Br	UR gas	308	2115	833	2127	871	578	369
GeH_3J	UR gas	248	2110	808	2121	854	558	369
$HSiF_3$	UR gas	2315	859	425	999	305	845	821
$HSiCl_3$	Ra fl	2258	489	250	587	179	799	273
$HSiBr_3$	Ra fl	2236	362	166	470	115	770	273
$HGeCl_3$	Ra fl	2159	409	181	438	149	699	273
$HGeBr_3$	Ra fl	2116	273	128	~325	95	674	273
HPO_3^{2-}	Ra, UR Lsg	2323	986	567	1085	462	1030	1124
HSO_3^-	UR krist $RbHSO_3$	2615	1045	630	1200	510	1135	1013
NSF_3	UR gas	1515	775	521	811	429	342	913
OPF_3	Ra fl	1395	875	476	982	476	337	272, 496
$OPCl_3$	Ra fl	1290	486	267	581	193	337	272
$OPBr_3$	Ra fl	1261	340	173	488	118	267	272
$OVCl_3$	Ra, UR fl	1035	409	164	504	131	249	401, 784
$OVBr_3$	UR fl	1025	271	120	400	83	212	777
SPF_3	Ra fl	695	854	440	940	402	276	271
$SPCl_3$	Ra fl	752	431	(247)	539	171	247	197, 272
$SPBr_3$	Ra fl	718	299	165	438	115	179	272
FPO_3^{2-}	Ra Lsg	795	1002	520	1136	520	379	730
FSO_3^-	Ra Lsg	786	1082	566	1287	592	409	424, 975, 990
$FClO_3$	UR gas	715	1061	550	1315	591	405	675, 715, 888
$FCrO_3^-$	UR krist $KCrO_3F$	635	912	338	952	370	257	299, 1058
$ClSO_3^-$	Ra Lsg	416	1050	535	1195	585	220	424
$ClCrO_3^-$	Ra Lsg	438	907	295	954	365	209	299, 1059
$ClReO_3$	Ra, UR fl	293	1001	435	961	344	196	781
$BrReO_3$	UR fl	195	997	350	963	332	168	781
SPO_3^{3-}	Ra Lsg	436	961	610	1037	519	367	1074
$S_2O_3^{2-}$	Ra Lsg	447	1004	670	1106	538	339	397, 989
$NOsO_3^-$	Ra Lsg	1021	897	309	871	372	309	673, 1197
$NReO_3^-$	UR krist $KReO_3N$	1025	909	—	936	—	—	206
$OH—ClO_3$	Ra, UR fl	742	1036	577	1230	577	430	vgl. Kap. III
$OH—SO_3^-$	Ra Lsg	887	1051	594	1200	594	429	
$OH—PO_3^{2-}$	Ra, UR Lsg	891	970	528	1082	528	389	
$OH—SeO_3^-$	Ra Lsg	742	866	394	920	394	322	

Polarisationsmessungen am *Ra*-Spektrum, auf die Rotationsstruktur der *UR*-Banden (symmetrische Kreisel) und auf die Untersuchung spektraler Übergänge. Die Zuordnung zu den Schwingungsformen ist nur dann gerechtfertigt, wenn die Schwingungen hinreichend charakteristisch sind.
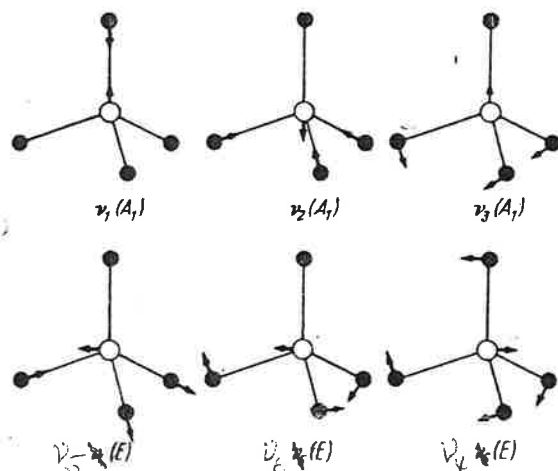

Die hier vorgenomme Nummerierung trifft für CH_3 nicht zu (siehe Herzberg) !/

Abb. 22. Schwingungsformen von Tetraedermolekülen ZXY_3 (C_{3v})

Dies ist meist der Fall mit Ausnahme von ν_1 und ν_3 des SiH_3F, $ClReO_3$ und $BrReO_3$, ν_4 und ν_6 von HPO_3^{2-} und HSO_3^- sowie ν_1 und ν_2 des SPF_3.

Untersucht wurden ferner die Spektren einer Reihe gemischter Halogenide von C, Si, Ge, Sn und Ti. Die Verbindungen von C und Si sind in reiner Form darstellbar, die von Ge, Sn und Ti treten jedoch nur

Tabelle 37. *Kraftkonstanten und Kernabstände von Tetraedermolekülen ZXY_3*

Molekül	$f(ZX)$	$f(XY)$	$r(ZX)$	$r(XY)$	Lit.
FCH_3	5,79	5,38	1,39	1,11	26
$ClCH_3$	3,42	5,48	1,78	1,10	26
$BrCH_3$	2,90	5,47	1,94	1,10	26
JCH_3	2,34	5,52	2,14	1,10	26
$FSiH_3$	5,32	2,77	1,59	1,48	295
$ClSiH_3$	2,98	2,81	2,05	1,48	295
$BrSiH_3$	2,45	2,81	2,21	1,48	295
$JSiH_3$	1,95	2,80	2,44	1,48	295
$FGeH_3$	4,21	2,67	1,73	1,52	369
$ClGeH_3$	2,56	2,67	2,15	1,52	369
$BrGeH_3$	2,12	2,66	2,30	1,55	369
$JGeH_3$	1,75	2,64	2,55		369
NSF_3	12,55	4,49	1,42	1,55	945
OPF_3	11,38	6,35	1,45	1,52	945
$OPCl_3$	9,98	2,45	1,45	1,99	989
$OVCl_3$	7,85	1,41			903
$SPCl_3$	4,14	2,49	1,85	2,02	989
$FClO_3$	3,91	9,41	1,66	1,45	945
$ClReO_3$	1,56	8,27	2,23	1,70	904

in Gemischen der entsprechenden Tetrahalogenide auf und sind hier ramanspektroskopisch entdeckt worden [274]. Unvollständige Spektren sind bekannt von BH_3F^- [21] und PSJ_3 ($\nu(PS) = 673$ [73]). Das für BF_3O^{2-} angegebene Spektrum [691] ist so ungewöhnlich, daß hier wohl eine Nachprüfung notwendig ist. Weiterhin wurden die UR-Spektren von $AsOF_3$ und $SbOF_3$ gemessen [263], vgl. auch Kap. III, S. 111. UR von gasförmigen VOF_3: 1060 (ν_1), 720 (ν_2), 805 (ν_4) [1228].

Für die meisten in Tab. 36 aufgeführten Moleküle liegen auch Kraftkonstantenberechnungen vor. Einige Ergebnisse für die hauptsächlich interessierenden Konstanten sind in Tab. 37 zusammengefaßt.

c) Y_2XZ_2, tetraederförmig (C_{2v})

Die Atomgruppen XY_2 und XZ_2 definieren je eine Symmetrieebene, deren Schnittlinie eine zweizählige Achse ist (Punktgruppe C_{2v}, vgl. Tab. 1, S. 16). Die Formen der neun Normalschwingungen sind in Abb. 23 dargestellt. ν_1, ν_2, ν_6 und ν_8 stellen danach Valenzschwingungen dar. ν_3 ist die Deformationsschwingung des Winkels XY_2, ν_4 entsprechend
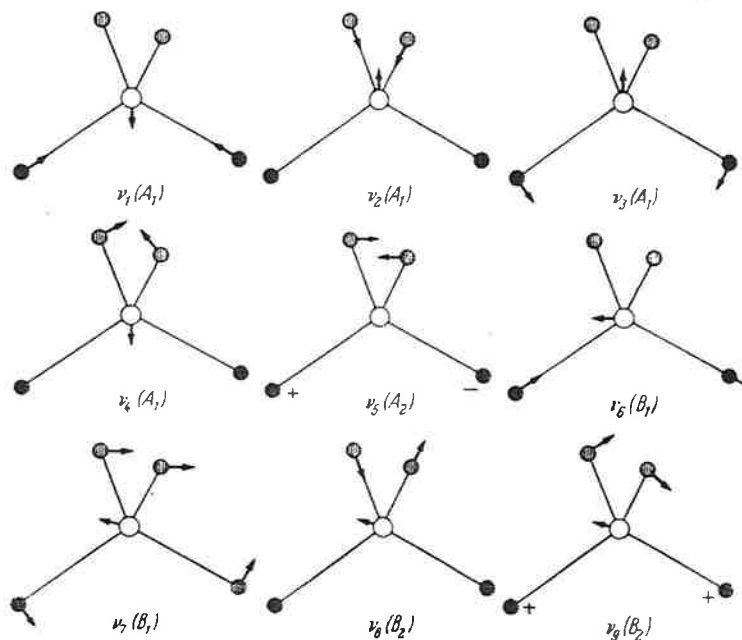

Abb. 23. Schwingungsformen von Tetraedermolekülen Y_2XZ_2 (C_{2v})

für XZ_2. Bei ν_5 werden die Gruppen XY_2 und XZ_2 symmetrisch zur Symmetrieachse gegeneinander verdreht, wobei das X-Atom fast in Ruhe bleibt. Solche Schwingungen werden als „Torsionsschwingungen" τ (im englischsprachigen Schrifttum „twisting") bezeichnet. Weitere Moleküle mit Torsionsschwingungen sind etwa die vieratomigen Ketten (s. S. 60) sowie X_2Y_4 und X_2Y_6 (s. S. 78, 84). ν_7 und ν_9

MOLECULAR SPECTRA

and

MOLECULAR STRUCTURE

II. INFRARED AND RAMAN SPECTRA OF POLYATOMIC MOLECULES

By

GERHARD HERZBERG, F.R.S.C.

National Research Council of Canada

It should be realized that in these cases, unlike the case of linear molecules, the l_i defined by (II, 282) do not in general represent the vibrational angular momenta about the symmetry axis. Rather, as we shall discuss in more detail in Chapter IV, section 2a, the vibrational angular momentum of a degenerate vibration v_i is $\zeta_i(h/2\pi)$, where ζ_i is in general non-integral and has a magnitude smaller than one.

It is clear from the preceding discussion that normal vibrations begin to lose their precise meaning when anharmonicities are large or when higher overtones are excited. Mecke (1006)(1007) pointed out that for the understanding of the observed higher vibrational levels of stretching vibrations involving H atoms (e.g. the C—H vibration in acetylene) a different starting point leads to a better understanding and a better representation. In this alternative (now called the local mode representation) one starts out from one local vibration (anharmonic), for example a C—H vibration, and its higher overtones and only afterwards introduces the relatively small interactions between the resulting levels of the equivalent vibrators. This point of view while dormant for some thirty years was taken up in 1968 by Henry and Siebrand (1008)(1009) for the higher vibrational levels of C_6H_6, by Scherer, Lehman and Klemperer (1010) for acetylene and by many other spectroscopists since then for a variety of molecules.

(c) Accidental degeneracy, Fermi resonance

Qualitative discussion. In a polyatomic molecule it may happen that two vibrational levels belonging to different vibrations (or combinations of vibrations) may have nearly the same energy, that is, may be *accidentally degenerate*. As was first recognized by Fermi (322) in the case of CO_2, such a "resonance" leads to a *perturbation of the energy levels* which is very similar to the vibrational perturbations of diatomic molecules (see Molecular Spectra I, p. 292f.). The only essential difference is that for diatomic molecules only vibrational levels of different electronic states can have nearly the same energy and thus perturb one another, whereas here two vibrational levels of the same electronic state can have the same energy and perturb each other. For example, in the case of CO_2 the level $v_1 = 0$, $v_2 = 2$, $v_3 = 0$ has almost the same energy as the level $v_1 = 1$, $v_2 = 0$, $v_3 = 0$, since $\nu_1 = 1337$ and $\nu_2 = 667$ cm^{-1} (see Table 41). For diatomic molecules, the perturbation is due to the interaction of vibration and electronic motion whereas here, for polyatomic molecules, the anharmonic terms in the potential energy, that is, the *interactions between different vibrations* are sufficient to produce a perturbation when two levels happen to lie very close together.

As for diatomic molecules, the two vibrational levels that have in zero approximation nearly the same energy *"repel"* each other and the actual levels do not follow accurately a formula of the type (II, 271) or (II, 281). Thus for CO_2 one of the two above-mentioned levels is shifted up and the other down so that the separation of the two levels is much greater than expected. At the same time a *mixing of the eigenfunctions* of the two states occurs. The deviation of the energy values from the formula and the mixing of the eigenfunctions is the stronger the smaller is the zero approximation difference of energy.

Mathematical formulation. In addition to depending, in an inverse way, on the "original" energy difference of the two levels, the magnitude of the perturbation (repulsion) depends, as for diatomic molecules, on the value of the corresponding *matrix element W_{ni} of the perturbation function W*:

$$W_{ni} = \int \psi_n^0 W \psi_i^{0*} d\tau. \tag{II, 289}$$

The perturbation function W is here essentially given by the anharmonic (cubic, quartic, $\cdots$) terms in the potential energy,[74] while $\psi_n{}^0$ and $\psi_i{}^0$ are the zero approximation eigenfunctions of the two vibrational levels that perturb each other. Since W, as we have seen above, has the full symmetry of the molecule (is totally symmetric), $\psi_n{}^0$ must have the same symmetry type as $\psi_i{}^0$ in order to give a non-zero value to W_{ni} and therefore to the magnitude of the perturbation. [If $\psi_n{}^0$ and $\psi_i{}^0$ had different symmetry type, the integrand of (II, 289) would change for at least one symmetry operation and therefore the integral would vanish.] Thus we have the important rule: *Only vibrational levels of the same species can perturb one another*, or, *Fermi resonance can occur only between levels of the same species*. This rule restricts very greatly the occurrence of vibrational perturbations (Fermi resonance) in symmetrical polyatomic molecules.

If the resonance is fairly close the *magnitude of the shift* can be obtained according to first-order perturbation theory (see texts on wave mechanics) from the secular determinant

$$\begin{vmatrix} E_n{}^0 - E & W_{ni} \\ W_{in} & E_i{}^0 - E \end{vmatrix} = 0, \tag{II, 290}$$

where $E_n{}^0$ and $E_i{}^0$ are the unperturbed energies. From this equation one obtains for the perturbed energy E, since according to (II, 289) $W_{in} = W_{ni}^{*}$,

$$E = \bar{E}_{ni} \pm \tfrac{1}{2}\sqrt{4|W_{ni}|^2 + \delta^2}, \tag{II, 291}$$

where $\bar{E}_{ni} = \tfrac{1}{2}(E_i{}^0 + E_n{}^0)$ is the mean of the unperturbed levels and $\delta = E_n{}^0 - E_i{}^0$ is the separation of the unperturbed levels.[75] Formula (II, 291) shows that there is no perturbation if $W_{ni} = 0$ and that, if δ is very small—that is, if the resonance is very close—the shift is $|W_{ni}|$ up for one and down for the other level. If δ is large compared to $2|W_{ni}|$, we can expand (II, 291) into

$$E = \bar{E}_{ni} \pm \left(\frac{\delta}{2} + \frac{|W_{ni}|^2}{\delta} \right), \tag{II, 292}$$

which is essentially the same as one would obtain from second-order perturbation theory applied to each level separately.

In Fig. 70 the position of the perturbed levels for a constant W_{ni} and $\bar{E}_{ni}$ is plotted as a function of δ, the separation of the unperturbed levels. The shift produced by the perturbation is given by
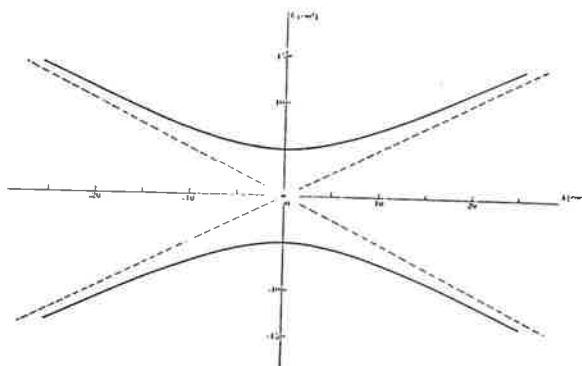

Fig. 70. Perturbation of two energy levels as a function of the separation of the unperturbed levels.—The broken lines represent the positions of the unperturbed levels, the solid curves those of the perturbed (actual) levels.

the separation of the heavy curve from the nearest of the broken lines (which represent the unperturbed levels). The shift is largest for $\delta = 0$, that is, for exact resonance.

[74] Strictly speaking, it also includes the deviation of the kinetic energy operator [see equation (II, 276)] from the form it has in the zero approximation used. But the corresponding contributions to W_{ni} are usually negligible for the perturbations here under consideration.

[75] Formula (II, 291) is seen to be identical with (V, 71) of Molecular Spectra I.

The *eigenfunctions* of the two resulting states can be shown to be (from standard methods of perturbation theory) the following mixtures of the zero approximation eigenfunctions $\psi_n{}^0$ and $\psi_i{}^0$:

$$\psi_n = a\psi_n{}^0 - b\psi_i{}^0,$$
$$\psi_i = b\psi_n{}^0 + a\psi_i{}^0, \tag{II, 293}$$

where

$$a = \left(\frac{\sqrt{4|W_{ni}|^2 + \delta^2} + \delta}{2\sqrt{4|W_{ni}|^2 + \delta^2}}\right)^{\frac{1}{2}}, \qquad b = \left(\frac{\sqrt{4|W_{ni}|^2 + \delta^2} - \delta}{2\sqrt{4|W_{ni}|^2 + \delta^2}}\right)^{\frac{1}{2}}. \tag{II, 294}$$

If $\delta = 0$ we obtain a fifty-fifty mixture; if δ is very large $\psi_n \rightarrow \psi_n{}^0$ and $\psi_i \rightarrow \psi_i{}^0$.

It should be emphasized that the perturbations are due to the same anharmonic terms in the potential energy that cause the terms $x_{ik}v_iv_k$ in the energy formula. The latter are due to the integrated perturbing effect of a large number of vibrational levels of which each contributes a term $|W_{ni}|^2/\delta$ as in (II, 292) whereas the former are due to the effect of one level that is particularly close to the one considered. Also, the terms $x_{ik}v_iv_k$ are always calculated by using as zero approximation the harmonic oscillator levels and eigenfunctions whereas for the perturbations one may instead also use the levels given by (II, 271) or (II, 281) and the corresponding eigenfunctions, to be substituted in (II, 289) and (II, 291).

In a way also the deviations of the characteristic group frequencies from their "normal" values in molecules containing several groups of similar frequencies may be considered as a special case of the vibrational perturbations, that is, if the "normal" values of these group frequencies are considered as the zero approximation. Also in this case such deviations occur only if the two or more vibrations have the same species and are always in such a direction as if they were produced by a "repulsion" (compare the discussion on p. 200).

Application to CO₂ and similar cases. As mentioned before, for CO_2 there is a very close resonance between the levels 1, 0, 0 and 0, 2, 0 since $2\nu_2$ happens to be very nearly equal to ν_1. The level 0, 2, 0 consists of two sublevels 0, 2^0, 0 and 0, 2^2, 0 with $l_2 = 0$ and 2, which have the species $\Sigma_g{}^+$ and Δ_g. According to the preceding discussion only the $\Sigma_g{}^+$ sublevel ($l_2 = 0$) can perturb the 1, 0, 0 level which has the species $\Sigma_g{}^+$ and conversely it alone is perturbed by the 1, 0, 0 level. This is shown in Fig. 71. The separation of the two levels 1, 0, 0 ($= 1388.3$ cm⁻¹) and 0, 2^0, 0 ($= 1285.5$ cm⁻¹) is much larger than would have been expected on the basis of the value for $\nu_2 (= 667.3$ cm⁻¹). Similarly, of course, the splitting of the two sublevels $l_2 = 0$ and $l_2 = 2$ of 0, 2, 0 is anomalously large (49.9 cm⁻¹). In consequence of the strong perturbation, a strong mixing of the eigenfunctions of the two levels 1, 0, 0 and 0, 2^0, 0 occurs so that the two observed levels can no longer be unambiguously designated as 1, 0, 0 and 0, 2^0, 0. Each actual level is a mixture of the two. Experimentally this mixing is evidenced by the occurrence of two strong Raman lines rather than one (see Chapter III).
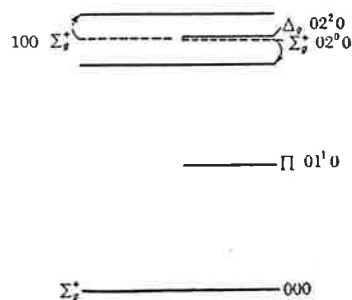

FIG. 71. Fermi resonance in CO₂. —The broken lines represent the unperturbed levels which go over, on account of the resonance, into the two levels to which the arrows point.

In consequence of the perturbation (resonance) between the levels 1, 0, 0 and 0, 2^0, 0 of CO_2, there are of course also perturbations between certain higher levels, for instance between 1, 0, 1 and 0, 2^0, 1 or between 1, 1^1, 0 and 0, 3^1, 0 or between the three levels 2, 0^0, 0; 1, 2^0, 0, and 0, 4^0, 0, and so on. A full discussion of these has been given by Adel and Dennison (37) [see also Dennison (280), and Chapter III, p. 275].

If the considerations of p. 205 are applied to linear symmetric XY_2, it is easily seen that the potential energy can only have the cubic terms

$$\alpha_{111}\eta_1{}^3 + \alpha_{122}\eta_1(\eta_{2a}{}^2 + \eta_{2b}{}^2) + \alpha_{133}\eta_1\eta_3{}^2. \tag{II, 295}$$

If this is substituted for W in (II, 289) and if for the eigenfunctions ψ_n^0 and ψ_i^0 products of harmonic oscillator functions (II, 53) and (II, 58) are used, it follows that W_{ni}, if n is a level $v_1 + 1$, v_2, v_3, and i is a level v_1, $v_2 + 2$, v_3, depends only on the potential constant α_{122}. None of the other cubic and none of the quartic terms gives a contribution. For the two levels 1, 0, 0 and 0, 2^0, 0 one finds

$$W_{100,\,02^00} = -\frac{h^{\frac{1}{2}}}{8\sqrt{2}\pi^3 c^{\frac{1}{2}}\omega_1^{\frac{1}{2}}\omega_2}\,\alpha_{122}.\tag{II, 296}$$

The value of W_{ni} for all other corresponding pairs of levels differs from $W_{100,\,02^00}$ only by a constant factor. Therefore the separation of all the resonating pairs can be represented by the two constants: δ (the unperturbed separation of the levels 1, 0, 0 and 0, 2^0, 0) and the interaction constant $W_{100,\,02^00}$. The two constants are therefore necessary in addition to the ω_i, x_{ik}, and g_{22} of (II, 287) for a complete representation of the vibrational energy levels of a linear symmetric XY_2 molecule such as CO_2 in which $\nu_1 \approx 2\nu_2$. For CO_2 Dennison (280) obtained the values $\delta = 16.7$ cm^{-1} and $W_{100,\,02^00} = 50.4$ cm^{-1}.[76]

A resonance phenomenon occurs *also in a classical treatment* of the vibrations. For example, for XY_2 during the perpendicular vibration ν_2 there is a slight force in the X—Y direction which has a maximum value twice during one period. This will lead to an excitation of the symmetrical oscillation ν_1 if its period is half as large as that of ν_2, that is, if $2\nu_2 = \nu_1$. Thus if at first only ν_2 is excited, after a while only ν_1 will be excited; and after a further interval only ν_2 will be excited, and so on. The situation is much the same as for two coupled pendulums. The motion may be considered as the superposition of two stationary vibrations of somewhat different frequencies.

If for a linear XY_2 molecule one had $\nu_1 \approx 3\nu_2$ or $2\nu_1 \approx 3\nu_2$, no perturbation would occur since none of the two sublevels of the state 0, 3, 0 with $l_2 = 1$ and 3 (Π_u and Φ_u state respectively) has the same species as the states 1, 0, 0, or 2, 0, 0 which are Σ_g^+ states.

Perturbations (Fermi resonances) similar to those observed for CO_2 have been found for a number of other molecules. They will be discussed briefly in Chapter III, when the vibrations of these molecules are considered. In all these cases a fundamental ν_i has nearly the same frequency as a first overtone, $2\nu_k$ of another vibration, or as a binary combination $\nu_k + \nu_l$ of two other vibrations. The mathematical treatment is very similar to that for XY_2 molecules. As above, such perturbations are only possible when the fundamental ν_i has the same species as one of the sublevels of $2\nu_k$ or $\nu_k + \nu_l$.

Application to H_2O. A somewhat different perturbation has been found to occur for H_2O by Darling and Dennison (263) and is probably of importance also for many other molecules. For H_2O the two vibrations ν_1 and ν_3 have a similar magnitude (3652 and 3756 cm^{-1}) but cannot perturb each other since they have different species. However, the two first overtones $2\nu_1$ and $2\nu_3$ have the same species (A_1) and therefore can perturb each other or, more generally, *any state v_1, v_2, v_3 with $v_1 > 2$ is perturbed by a state $v_1 - 2$, v_2, $v_3 + 2$*. The recognition of this effect by Darling and Dennison (263) has first led to a satisfactory analysis of the vibration spectrum of H_2O (see Chapter III).

The essential difference from the case of CO_2 is that here the matrix element W_{ni} would be zero if only cubic terms of the potential energy were taken into account and harmonic oscillator functions were used for ψ_n^0 and ψ_i^0. However, the quartic terms of the potential with harmonic oscillator functions and the cubic terms with anharmonic oscillator functions give each a contribution. Darling

---

[76] Our $W_{100,\,02^00}$ is Dennison's $\dfrac{-b}{\sqrt{2}}$. His constant b corresponds to our α_{122} for a certain choice of dimensionless normal coordinates.

calculations by Dennison and Johnston (283) and Dennison (280). They have predicted the frequencies of the intermediate methanes from those of CH_4 and CD_4 by computing the most general potential constants of CH_4 and using these same constants in deriving the frequencies of CH_3D, CH_2D_2, CHD_3 with the help of formulae developed by Rosenthal (747). However, for a few fundamentals these authors have not taken the correlation rules into account. This has been done throughout in Table 82. In place of the potential calculations one could also have used the isotope relations [for example equation (II, 330)] to find the correct correlation. It may be left to the reader to check whether they are actually fulfilled.

Childs and Jahn (207) have observed a photographic infrared band of CH_3D of the ∥ type at 9020.8 cm^{-1}, which is probably one of the sub-bands of the second overtone of 3030.2 cm^{-1}. Bovey (1076) has observed two photographic infrared bands of CHD_3 at 8623 and 11267 cm^{-1}. For more recent work including local mode interpretation see Voth, Marcus and Zewail (1077).

Carbon tetrachloride, CCl_4. The Raman spectrum of liquid CCl_4 has been investigated by a large number of workers [see Kohlrausch (13) (14)], but no one seems to have investigated the spectrum of the vapor in any detail. The infrared spectrum has been investigated by only a few authors [most recently by Schaefer and Kern (766) and Barchewitz and Parodi (101)] and also only for the liquid state.[118] It seems fairly safe, however, to assume that the difference between the spectrum of the vapor and that of the liquid is slight in view of the symmetrical, inert character of the molecule.

Considering the similarity to CH_4, it seems natural to assume that CCl_4 also has the *symmetrical tetrahedral structure* (point group T_d). But at some times this has been doubted by various investigators of the spectrum. We shall see, however, that more recent investigations definitely support the tetrahedral model.

The Raman spectrum yields the eight displacements given in Table 83, some of which occur both as Stokes and as anti-Stokes lines (see Fig. 77). Three of the shifts, 145, 434, and 1539 cm^{-1}, correspond to exceedingly weak Raman lines. They are in all probability overtone or combination bands and are indeed very readily interpreted as such (see Table 83). Moreover, a frequency as high as 1539 would not be expected as a fundamental of CCl_4, the vibration frequency of diatomic CCl being 844 cm^{-1}. Thus there remain four or five observed Raman-active fundamentals, depending on whether the two lines 762.0 and 790.5 cm^{-1} are considered as a doublet or as two distinct frequencies. The first assumption is in agreement with the tetrahedral model since for it just four fundamentals, all active in the Raman effect, should occur. Furthermore, as it should be for the tetrahedral model, one of the Raman lines (with $\Delta \nu = 460$ cm^{-1}) is almost completely polarized, whereas the other three are completely depolarized (see p. 270f.). Finally, the infrared spectrum seems to show only two fundamentals, the band 305 cm^{-1} and the doublet band 775 cm^{-1}, in agreement with expectation for the tetrahedral model. While the Raman fundamental 218 cm^{-1} is probably outside the range investigated in the infrared, the Raman band 460 cm^{-1} is certainly within this range and is definitely absent. In consequence of this observation and in view of the complete polarization[119] in the Raman effect, this fundamental must be considered as the totally symmetric vibration $\nu_1(a_1)$. The two infrared-active fundamentals 775 and 305 cm^{-1} can only be $\nu_3(f_2)$ and $\nu_4(f_2)$ respectively (see Fig. 41), and thus the fourth Raman-active fundamental at 218 cm^{-1} must be $\nu_2(e)$. All of the numerous other infrared bands of liquid CCl_4 found by Schaefer and Kern can be interpreted on the basis of these four fundamentals (see Table 83). The doublet structure of ν_3 is explained in this interpretation without difficulty as due to a Fermi resonance [Placzek (700)] between ν_3 and $\nu_1 + \nu_4$. As can be seen from Table 83, the upper state of $\nu_1 + \nu_4$ has nearly the same energy as the average of the two doublet components and also has the same species (F_2) as the upper state of ν_3.

Langseth (547) found a fine structure of the Raman lines ν_1, ν_2, and ν_4 of CCl_4, which he thought was due to a deviation from tetrahedral symmetry. But Wu and Sutherland (957) have shown that this fine structure can be explained as due to a partly resolved isotope effect produced by the presence of the isotopic modifications CCl_4^{35} (31.6 per cent), $CCl_3^{35}Cl^{37}$ (42.2 per cent) and $CCl_2^{35}Cl_2^{37}$ (21.1 per cent).[120] This has been further confirmed by intensity measurements in the fine structure carried out by Menzies (621).

---

[118] Schaefer and Kern (766) state that for the most intense bands they used also the vapor but do not give separate measurements.

[119] If the slight observed depolarization of 5 per cent is real it can easily be explained [see Placzek (700)] as due to the effect of the isotopes $CCl_3^{35}Cl^{37}$ and $CCl_2^{35}Cl_2^{37}$, for which the polarizability change is not exactly spherically symmetric.

[120] The molecules $CCl^{35}Cl_3^{37}$ (4.7 per cent) and CCl_4^{37} (0.4 per cent) are not abundant enough to produce a noticeable contribution.

While thus all observations are in agreement with the symmetrical tetrahedral model, it is necessary to inquire whether they are not also in agreement with a less symmetrical model. As in the case of CH_4 (see above), the plane symmetrical structure (point group D_{4h}) is immediately ruled out by the fact that one of the fundamentals (775 cm^{-1}) occurs in the infrared as well as the Raman spectrum.[121] Two other conceivable models are a pyramid with the C atom at the vertex (point

TABLE 83. RAMAN SPECTRUM AND PART[123] OF THE INFRARED SPECTRUM OF LIQUID CCl_4.

Raman shifts[124] $\Delta\nu_{vacuum}$, (cm^{-1})	Infrared[125] bands ν_{vacuum}, (cm^{-1})	Assignment[126]	References
145 v.w.		$\nu_1-\nu_4[F_2]$	(43)
217.9 s. depol.		$\nu_2(e)$	(547)
314.0 s. depol.	305	$\nu_4(f_2)$	(547) (819) (101)
434 v.w.		$2\nu_2(A_1+E)$	(43)
$\left.\begin{array}{c}455.1 \\ 458.4 \\ 461.5\end{array}\right\}$ v.s. pol.		$\left.\begin{array}{l}CCl_2{}^{35}Cl_2{}^{37} \\ CCl_3{}^{35}Cl^{37} \\ CCl_4{}^{35}\end{array}\right\}\nu_1(a_1)$	(547) (547) (547)
	635 w.	$2\nu_4(A_1+E+F_2)$	(766)
762.0 m. depol.	$\left.\begin{array}{l}768 \text{ v.s.} \\ 797 \text{ v.s.}\end{array}\right\}$	$\nu_3(f_2), \nu_1+\nu_4(F_2)$	(547) (766)
790.5 m. depol.			(547) (766)
	$\left.\begin{array}{l}982 \text{ m.} \\ 1006 \text{ m.}\end{array}\right\}$	$\nu_2+\nu_3(F_2), \nu_1+\nu_2+\nu_4(F_2)$	(766) (766)
	$\left.\begin{array}{l}1068 \text{ w.} \\ 1107 \text{ w.}\end{array}\right\}$	$\nu_3+\nu_4(A_1+E+F_2), \nu_1+2\nu_4(A_1+E+F_2)$	(766) (766)
	$\left.\begin{array}{l}1218 \text{ m.} \\ 1253 \text{ m.}\end{array}\right\}$	$\nu_1+\nu_3(F_2), 2\nu_1+\nu_4(F_2)$	(766) (766)
	1529 m.	$2\nu_3(A_1+E+F_2)$	(766)
1539 v.w. pol.[127]	$\left.\begin{array}{l}1546 \text{ s.} \\ 1575 \text{ m.}\end{array}\right\}$	$2\nu_1+2\nu_4(A_1+E+F_2)$ $\nu_1+\nu_3+\nu_4(A_1+E+F_2)$	(710) (766) (766)

group C_{4v}) or a pyramid with an H atom at the vertex and the C atom on the axis (point group C_{3v}, for example, when there is only a slight deviation from tetrahedral symmetry, as has at one time been assumed). These models would have the fundamentals $2A_1 + 2B_1 + B_2 + 2E$ and $3A_1 + 3E$ respectively (see Table 36), all of which would be Raman active (see Table 55). Apart from the fact that the number of observed reasonably strong Raman lines would be less than the number of Raman active fundamentals (even if the doublet at 775 is counted as two fundamentals), the important point is that only one polarized Raman shift (460 cm^{-1}) occurs, whereas for the above two models two or three should occur and they should also be the strongest Raman lines. Furthermore, in the case of the model of symmetry C_{3v}, if the doublet 775 is counted as two lines [122] the number of depolarized Raman lines is four instead of the three required ones. Thus we can consider also the models of symmetry C_{3v} and C_{4v} as ruled out. For still less symmetrical models, the number of

[121] The fact that both components (762 and 790 cm^{-1}) occur in both cases excludes the possibility of a chance coincidence.

[122] Otherwise there would be no reason to assume any other but the tetrahedral model.

[123] Only the part below 1600 cm^{-1} and only bands with an absorption coefficient $k_{maximum} > 4$ are given.

[124] For the degree of depolarization see Rao (717) and the literature quoted by him.

[125] Barchewitz and Parodi (101) give in addition the bands at 217?, 529, 370, 247 cm^{-1} observed in paraffine solution.

[126] Sublevels of species F_1 are omitted, since they combine with the ground state neither in the Raman nor in the infrared spectrum.

[127] Polarization from Rao (718).

polarized Raman lines would *a fortiori* not be correct, so we can consider the symmetrical tetrahedral model as proven.

It should not be overlooked that the following difficulty, which is independent of the CCl_4 model assumed, still remains to be solved: Since the fundamental frequencies of CCl_4 are small, a considerable fraction of the molecules is in the states in which one (or even more than one) vibration is excited by one or two quanta. This gives rise to comparatively strong anti-Stokes lines, as observed for CCl_4. It should also give rise to certain *difference bands* in the Raman spectrum, which however have not been observed. While the ordinary difference bands such as $\nu_1 - \nu_2$, $\nu_3 - \nu_2$, $\cdots$ would be expected to be very weak, just as other binary combinations, and therefore are not readily observed (only one such band, $\nu_1 - \nu_4 = 145$ cm^{-1}, has been found for CCl_4), there are others such as $\nu_1 + \nu_2 - \nu_2$, $2\nu_2 - \nu_2$, $\cdots$ whose intensity, apart from the Boltzmann factor, should be of the same order of magnitude as that of the fundamentals ν_1, ν_2, $\cdots$ respectively. In general, these difference bands coincide very nearly with the corresponding fundamentals and are therefore not resolved in Raman measurements, but in the case of perturbations (Fermi resonance) some of them will be widely separated from the fundamentals. In the present case the transition $\nu_1 + \nu_4 - \nu_4$ whose upper state is split because of resonance, should consist of the two lines at $790.5 - 314.0 = 476.5$ cm^{-1} and $762.0 - 314.0 = 448.0$ cm^{-1}, which would be well separated from ν_1. According to calculations by Horiuti (457), they should have about $\frac{1}{5}$ of the intensity of the strong line 460 cm^{-1}. That they have not been found may be due to the fact that these difference lines are much broader than the main line. But more experimental data, particularly for CCl_4 vapor and with long exposure times, are required to clear up this point.

For a discussion of the force field in CCl_4 see Tables 39 and 46 and the accompanying discussion.

Methyl chloride, CH_3Cl. Since, as has been shown, CH_4 is a symmetrical tetrahedral molecule one would expect CH_3Cl to have a *three-fold axis of symmetry* (the C—Cl axis); that is one would expect it to belong to point group C_{3v}. This conclusion is confirmed by the investigation of the vibrational spectrum and particularly of the rotational fine structure (see Chapter IV). The symmetrical model (C_{3v}) has six fundamentals, three totally symmetric ones (A_1) and three degenerate ones (E), all of which are both infrared and Raman active, whereas any less symmetric model would give nine active fundamentals. Actually the infrared as well as the Raman spectrum can be analyzed in terms of six fundamentals (see Table 84). Unfortunately, with one exception (see Table 84), the Raman spectrum has been investigated only for *liquid* CH_3Cl [first by Dadieu and Kohlrausch (256)], while the infrared data refer to the gaseous state [first studied by Bennett and Meyer (138)]. Slight inconsistencies are due to this fact.

The form of the six normal vibrations is represented in Fig. 91. The totally symmetric vibrations ν_1, ν_2, ν_3 (species A_1) give rise to $\parallel$ bands in the infrared (only $M_z \neq 0$; see Table 55), the degenerate vibrations ν_4, ν_5, ν_6 give rise to $\perp$ bands ($M_z = 0$). Actual observation shows that there are indeed three $\parallel$ and three $\perp$ bands [128] by whose combinations all other bands can be explained. In addition it is found, in agreement with theoretical expectation, that the Raman lines corresponding to the $\parallel$ bands are polarized, those corresponding to the $\perp$ bands are depolarized. To be sure there are four strong $\parallel$ bands in the infrared which might be considered as fundamentals, but two of them at 2878.8 and 2966.2 cm^{-1} form a fairly close doublet whose center coincides very nearly with twice the wave number of the $\perp$ band at 1453.2 cm^{-1}. It can therefore be concluded that a Fermi resonance occurs [Adel and Barker (36)] and that the doublet corresponds to one fundamental only (see below).

More detailed calculations show, in agreement with what has been said about group frequencies in Chapter II, section 4f, that the two vibrations ν_1 and ν_4 of frequency about 3000 cm^{-1} are essentially C—H stretching vibrations, that the lowest $\parallel$ vibration ν_3 is essentially a C—Cl vibration, that the lowest $\perp$ vibration ν_6 is essentially a $H_3{\equiv}C$—Cl bending vibration, and that the two intermediate vibrations are essentially CH_3 deformation vibrations (see Fig. 91). The observed Cl isotope effect is also in agreement with this assignment, at least for the $\parallel$ bands. The largest isotope shift, of 6 cm^{-1} occurs for ν_3, the C—Cl vibration [Barker and Plyler (111)]. A much smaller shift, of 0.8 cm^{-1}, has been observed for ν_2 [Nielsen and Nielsen (659)], and the shift for ν_1 is smaller than the resolution used for this band (that is, smaller than 0.8 cm^{-1}). The shift for ν_3 agrees well with the one calculated by considering CH_3Cl as a diatomic molecule CH_3—Cl.

The observed overtone and combination bands of CH_3Cl are given together with the fundamentals in Table 84. All but two very weak Raman shifts 2683 and 1106 cm^{-1} are readily explained

---

[128] How they are distinguished will be explained in the next chapter.

TABLE 84. INFRARED AND RAMAN SPECTRA OF CH_3Cl.[129]

ν_{vacuum} (cm⁻¹) Infrared (vapor)	$\Delta\nu_{vacuum}$ (cm⁻¹) Raman[130] (liquid)	Assignment[131]	References	ν_{vacuum} (cm⁻¹) Infrared (vapor)	Assignment[131]	References	ν_{vacuum} (cm⁻¹) Infrared (vapor)	Assignment	References
732.1 || (v.s.)	709 (v.s. pol.)	ν_3 CCl (a_1)	(138)	3978.9[133] $\perp$	$\nu_1 + \nu_6 (E)$	(655)	6894 ?	$\nu_1 + \nu_4 + \nu_6,\ 2\nu_1 + \nu_6$	(634)
			(111)	4046.0[133] ||	$\nu_4 + \nu_6 (A_1 + [A_2] + E)$	(655)	8690 P.I. (m.)	$3\nu_1 (A_1)$	(846)
1015.0[132] $\perp$ (m.)	1016 (w. depol.)	$\nu_6 (c)$	(138)				8890 P.I. (w.)	$2\nu_1 + \nu_4 (E)$	(846)
	1106 (w.)	?		4088.4[133] ||	$\nu_2 + 2\nu_6 (A_1 + E)$	(655)	8990 $\perp$ P.I. (v.w.)	$\nu_1 + 2\nu_4 (A_1 + E)$	(898) (846)
1354.9 || (s.)	1370 (v.w. pol.)	ν_2 CH$_3$ (a_1)	(138)	4174.7 $\perp$		(655)	9155 P.I. (v.w.)	$3\nu_4 (A_1 + [A_2] + E)$	(846)
			(655)	4229.4 ||	$\nu_1 + \nu_2 (A_1)$	(655)	9690 P.I. (v.w.)	$3\nu_1 + \nu_6 (E)$	(846)
1454.6[132] $\perp$ (m.)	1446 (w. depol.)	ν_5 CH$_3$ (e)	(138)	4382.6 $\perp$	$\nu_4 + \nu_2 (E)$	(655)	10050 P.I. (v.w.)	$3\nu_1 + \nu_2,\ 3\nu_4 + \nu_6,\ \cdots$	(655) (846)
2461.0 $\perp$ (w.)		$\nu_5 + \nu_6 (A_1 + [A_2] + E)$	(655)	4452.3 $\perp$	$\nu_4 + \nu_5 (A_1 + [A_2] + E)$	(655)	11239 ? P.I. (w.)	$4\nu_1,\ 3\nu_1 + \nu_4$	(846) (901)
									(864)
	2683 (v.w.)	$2\nu_2 (A_1)$?		5400 $\perp$	$\nu_2 + \nu_4 + \nu_6$?	(655)	11265 || P.I. (w.)	$2\nu_1 + 2\nu_4,\ \nu_1 + 3\nu_4,\ 4\nu_4$	(901) (846)
	2815 (w.)	$\nu_2 + \nu_5 (E)$		5900 $\perp$	$\nu_4 + \nu_1,\ \nu_4 + 2\nu_5$	(655)	13800[133] P.I. (v.w.)	$5\nu_1,\ 4\nu_1 + \nu_4,\ \cdots$	(655)
2878.8 || (s.)	2861 (m.)	$2\nu_5 (A_1 + E)$	(138)	6013.5[133] ||	$2\nu_4 (A_1 + E)$	(655)			
2966.2 || (v.s.)	2955 (v.s. pol.)	ν_1 CH (a_1)	(138)	6076[133] $\perp$		(655)			
3041.8[132] $\perp$ (s.)	3036 (m. depol.)	ν_4 CH (e)	(138)						

[129] Wherever the bands of CH_3Cl^{35} and CH_3Cl^{37} are resolved the data given refer to the former.

[130] The Raman data given are due to Wagner (906). References to the numerous earlier papers on the Raman spectrum of CH_3Cl may be found in Kohlrausch (13) (14) and Hibben (10). More recently Nielsen and Ward (670) have observed two Raman shifts 726 and 2968 cm⁻¹ for the vapor. These agree much better than the corresponding Raman shifts of the liquid with the infrared spectrum of the vapor.

[131] The numbering is that used in Fig. 91, which is different from that used by Barker, Dennison, and their co-workers. The symbols in parentheses give the species of the upper states. Transitions to the substates A_2 are not allowed (see Table 55). This has been overlooked by Nielsen and Barker (655). Consequently their interpretation of the overtones has been slightly changed. In the designation of the overtones, $2\nu_5$ has been taken for the lower, ν_1 for the higher of the two resonating levels.

[132] The position of the zero line in these bands is incorrectly given in all papers on the subject. It is not the frequency of the line $n = 0$ in Bennett and Meyer's (138) nomenclature but approximately half-way between the lines $n = 0$ and $n = -1$. It is exactly half-way between these lines only if $\zeta = 0$ and $A' = A''$, $B' = B''$ (see Chapter IV, section 2b). The deviation because of $\zeta \neq 0$ has been taken into account in the above table only for the fundamentals.

[133] There are a few inconsistencies in the last two decimal places of these figures in Nielsen and Barker's paper which have been corrected as far as possible.

in terms of the above fundamentals. The Raman shift 2683 may be $2\nu_2$, but a reasonable explanation for the shift 1106 cannot be given. Possibly it might be related to the fact that the Raman spectrum refers to liquid rather than gaseous CH_3Cl and that in the liquid double molecules occur.

The resonance between $2\nu_5$ and ν_1 mentioned above influences, of course, only the sublevel A_1 of $2\nu_5$ whereas $2\nu_5(E)$ remains uninfluenced.[134] That is why only two strong $\parallel$ bands appear in this region but no $\perp$ band of comparable intensity. It should also be noted that the resonance is not very close as indicated by the unequal intensities of the Raman and infrared bands.
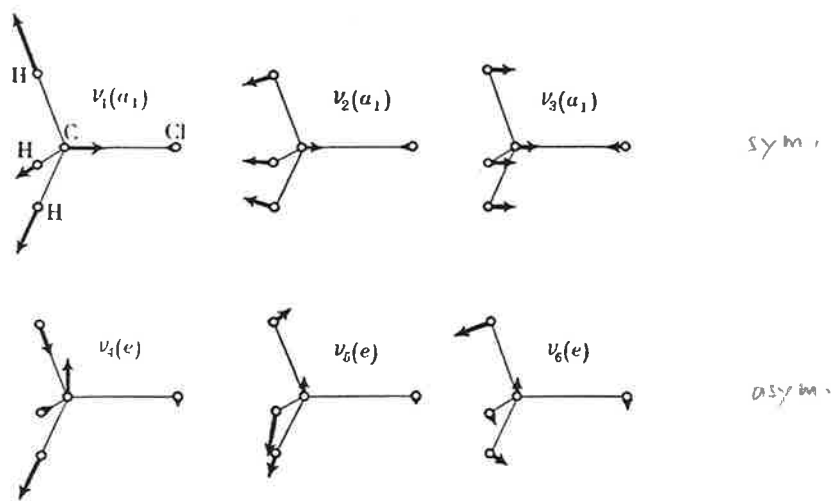
Fɪɢ. 91.   Normal vibrations of CH_3Cl (schematic).—Only side views, and only one component of each degenerate vibration are given.

It is interesting that for some of the overtone and combination bands (for example $2\nu_4$) at least two of the sublevels of the upper state give rise to sub-bands as indicated in Table 84. The complicated structure of the photographic infrared bands is probably due to the overlapping of several such sub-bands as well as to the approximate equality of ν_1 and ν_4, and to the isotope effect.

Slightly different values for the fundamental frequencies are given in Table 69 of vol. III. Among the extensive modern literature about the CH_3Cl molecule we refer to (1078) (1079) (1080) (1081) (1082) (1083).

CH_3F, CH_3Br, CH_3I, CD_3Cl, CD_3Br.   The other methyl halides have not been investigated quite as fully as CH_3Cl. Naturally their spectra are very similar to that of CH_3Cl. We can therefore omit a full discussion and give in Table 85 only the fundamental frequencies according to Bennett and Meyer (138) and Barker and Plyer (111). Data about overtone and combination bands are given by Moorhead (634), Vierling and Mecke (901), Verleger (898), Naudé and Verleger (650), and Thompson (846). For a discussion of the Raman spectra of the liquids see Wagner (906) and the books of Kohlrausch (13) (14) and Hibben (10). The Raman spectrum of CH_3Br vapor has been investigated by Nielsen and Ward (670). The fundamentals of "heavy" methyl chloride and bromide (CD_3Cl and CD_3Br) recently obtained by Noether (672) are also included in Table 85. The Fermi resonance discussed above for CH_3Cl occurs also for the other molecules. Therefore both resonating levels have been given in Table 85. As for CH_3Cl, the high-frequency component of the doublet is from two to four times as strong as the low-frequency component, indicating that the unperturbed ν_1 is nearer the larger of the two frequencies.

It is interesting to study the way in which the frequencies change in going from the lighter to the heavier halides. For this purpose Fig. 92 gives a graphical representation of the four spectra. It is seen that the frequencies ν_1, ν_4, ν_5 are remarkably constant throughout the series of molecules

---

[134] It may be noted that $2\nu_3$ very nearly equals ν_5 but no perturbation occurs because the states have different species.

TABLE 85. FUNDAMENTAL FREQUENCIES OF THE METHYL HALIDES,[135] AFTER BENNETT
AND MEYER (138), BARKER AND PLYLER (111), AND NOETHER (672).

	ν_{vacuum} (cm^{-1})					
	CH_3F	CH_3Cl^{35}	CH_3Br^{79}	CH_3I	CD_3Cl	CD_3Br
$\nu_3(a_1)$	1048.2	732.1	611	532.8	695	577
$\nu_6(e)$	1195.5	1015.0	952.0	880.1	775	717
$\nu_2(a_1)$	1475.3	1354.9	1305.1	1251.5	1029	987
$\nu_5(e)$	1471.1	1454.6	1445.3	1440.3	1058	1053
$2\nu_5(A_1)$	2361.6	2878.8	2861	2861	2103	2088
$\nu_1(a_1)$	2964.5	2966.2	2972	2969.8	2161	2151
$\nu_4(e)$	2982.2	3041.8	3055.9	3060.3[136]	2286	2293

CH_3X. This is in agreement with their interpretation as C—H vibrations and also follows directly from calculations in which a pure valence force system is assumed [see Wagner (906)] as well as when a somewhat more general force system is assumed [Slawsky and Dennison (796), Linnett (582)]. The frequency ν_3 decreases considerably in going from CH_3F to CH_3I in agreement with the assumption that it is a C—X vibration, and similarly the bending vibration ν_6 decreases although
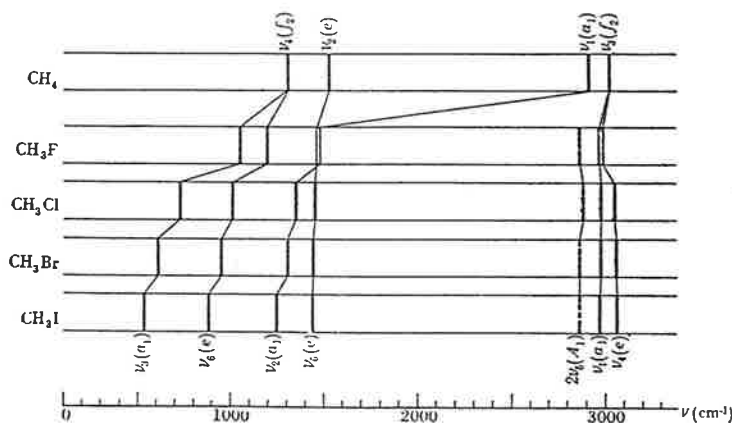

FIG. 92. Observed fundamental vibration spectra of the methyl halides and methane.—The broken lines indicate the frequencies $2\nu_5(A_1)$ which are in resonance with $\nu_1(a_1)$. The unperturbed ν_1 would be between ν_1 and $2\nu_5$ (see text).

not quite as strongly. These changes are easily understood on the basis of the change in mass alone (the change of the C—X force constant acts in the same direction). However, the cause of the appreciable change of the symmetrical C—H bending vibration ν_2 is perhaps less easily visualized. The reason for this change is that ν_3, which has the same species, pushes ν_2 upward. If for a moment we consider the CH_3 group as one atom, then ν_3 would increase up to about 3000 cm^{-1} if we were to decrease the atomic weight of X to 1; that is, the curves ν_3 and ν_2 as functions of the mass would intersect each other. Actually, such an intersection does not take place because of the mechanical

---

[135] The frequencies of the degenerate fundamentals have been corrected as indicated in footnote 132 on p. 313 including the correction due to ζ. All frequencies have been corrected for vacuum. The numbering is that of Fig. 91.

[136] This is the value given by Lagemann and Nielsen (546) (but corrected for vacuum and for the effect of ζ), Bennett and Meyer's numbering of the fine structure lines being incorrect in this case.

coupling of the motions of the different atoms (the cross terms in the kinetic energy). In actual fact the CH_3 deformation frequency ν_2, if we could continuously decrease the mass of X, would eventually go over into the valence stretching vibration $\nu_1 = 2914$ cm^{-1} of methane, whereas the C—X stretching frequency ν_3 (together with ν_6) would go over into the deformation frequency ν_4 of methane [see particularly Wagner (906)]. This is shown in Fig. 92.

The preceding considerations supply a good example for the previous discussion of the limitations of the concept of group frequencies (see p. 199f.). A frequency will remain constant in a series of molecules containing the same group (or groups) and can be assigned to that group only *as long as no other frequency belonging to a normal mode of the same species is in its neighborhood*. This condition is well fulfilled for ν_1, ν_4, ν_5 in all halides (and even in CH_4) but for ν_2 and ν_3 only for the heavy halides. For CH_3I, ν_3 may well be called the C—I vibration frequency and ν_2 the symmetrical CH_3 deformation frequency, but the corresponding statement for CH_3F would have much less significance.

Chloroform, $CHCl_3$. The infrared spectrum of chloroform is only very incompletely known. Most of the work has been limited to the investigation of liquid (or dissolved) $CHCl_3$ with low dispersion particularly in the region of the fundamentals. [Emschwiller and Lecomte (304) and Barchewitz and Parodi (101)]. While a number of overtone and combination bands have been observed in the shorter-wave-length region, including the photographic infrared [Ellis (302), Timm and Mecke (864), Vierling and Mecke (901), Maione (595), Corin (231), Carrelli and Tulipano (194), Rumpf and Mecke (751), Herzberg and McKay (436)], we give in Table 86 only the fundamentals. But it should be mentioned that the series of overtone bands of the C—H stretching vibration has been observed to $v = 6$ far into the visible region [Ellis (302), Rumpf and Mecke (751)]. The series is (in the liquid)

$$3019, \quad 5900, \quad 8700, \quad 11315, \quad 13860, \quad 16300 \text{ cm}^{-1}.$$

The reason why this series stands out so clearly here in contrast to many other cases is that there is only one C—H stretching vibration, which has a much larger frequency than all the other fundamentals.

TABLE 86.   FUNDAMENTAL FREQUENCIES OF $CHCl_3$ AND $CDCl_3$.

Assignment	CHCl₃			CDCl₃
	Infrared, ν_{vacuum} (cm^{-1})	Raman		Raman
		Liquid, Wood and Rank (954)[137] $\Delta\nu_{vacuum}$ (cm^{-1})	Vapor, Nielsen and Ward (670) $\Delta\nu_{vacuum}$ (cm^{-1})	Liquid, Wood and Rank (954)[137] $\Delta\nu_{vacuum}$ (cm^{-1})
ν_6 C Cl₃(c)	260[138]	262.0 (v.s. depol.)	261	262.0 (v.s.)
ν_3 C Cl₃(a_1)	364[138]	365.9 (s. pol.)	363	366.5 (s.)
ν_2 C Cl(a_1)	667[139]	668.3 (s. pol.)	672	650.8 (s.)
ν_5 C Cl(c)	760[139]	761.2 (s. depol.)	760	737.6 (s.)
ν_4(c)	1205[139]	1215.6 (m. depol.)	1217	908.3 (m.)
ν_1 CH(a_1)	3033[140]	3018.9 (s. pol.)	3030	2256.0 (s.)

The Raman spectrum of liquid $CHCl_3$ has been investigated by many investigators [for detailed references see Kohlrausch (13) (14) and Hibben (10)] and recently also the spectrum of the vapor by Nielsen and Ward (670). There are six strong Raman shifts, as given in Table 86. In addition, a very weak line occurs for the liquid with a shift of 1505 cm^{-1} very probably corresponding to the first overtone of the band 761.2 cm^{-1}. Thus the number of Raman fundamentals is in agreement with that expected on the symmetrical (C_{3v}) model. Furthermore, three of the strong Raman bands

[137] Independent values of similar accuracy have been obtained by Redlich and Pordes (731a).

[138] Measured by Barchewitz and Parodi (101) in $CHCl_3$ dissolved in paraffine.

[139] Measured by Emschwiller and Lecomte (304) in liquid $CHCl_3$.

[140] Measured by Ginsburg, according to a footnote in Voge and Rosenthal (903), in $CHCl_3$ vapor.

are partly polarized, the other three completely depolarized [see (191) and Fig. 82, p. 270], as should be the case. Thus, as in the case of the methyl halides, the first three can be assigned to ν_1, ν_2, ν_3, the other three to ν_4, ν_5, ν_6 in order of decreasing frequency. Further confirmation of this assignment is obtained if the fundamental frequencies of $CHCl_3$ are calculated by assuming the same force constants as in CH_4, CH_3Cl, and CCl_4. This has been done by Voge and Rosenthal (903), who found very satisfactory agreement with the observed frequencies. Finally, the Raman spectrum of "heavy" chloroform $CDCl_3$ has also been investigated and is included in Table 86. The fundamentals of $CDCl_3$ observed in this way also agree with those predicted from the force constants [Voge and Rosenthal (903)].

Most of the fundamental frequencies of $CHCl_3$ may be ascribed fairly definitely to certain bonds or groups (see Fig. 91 and Table 86). ν_1 is without doubt essentially a C—H stretching vibration. ν_2 is essentially the symmetrical C—Cl stretching vibration (corresponding to ν_3 of CH_3Cl) and ν_5 the corresponding degenerate frequency. ν_3 and ν_6 are the symmetrical and degenerate CCl_3 deformation vibrations and finally ν_4 is the bending vibration of the C—H group against the rest of the molecule. In agreement with this interpretation, the isotope shifts for $CDCl_3$ are practically zero for ν_3 and ν_6, are small for ν_2 and ν_5 but very large for ν_1 and ν_4.

Methylene chloride, CH_2Cl_2. There can hardly be any doubt, considering the structures of CH_4, CH_3Cl, $CHCl_3$, CCl_4, that methylene chloride has a tetrahedral structure of point group C_{2v} (similar to CH_2D_2, see above). The infrared and Raman data thus far available do not contradict this assumption but they are hardly sufficient to prove it definitely. Besides, the assignment of

TABLE 87. INFRARED [141] AND RAMAN SPECTRA OF LIQUID CH_2Cl_2 AFTER
CORIN AND SUTHERLAND (233) AND WAGNER (908).

Assignment[142]	Infrared ν_{vacuum} (cm^{-1})	Raman $\Delta\nu_{vacuum}$ (cm^{-1})	Assignment[142]	Infrared ν_{vacuum} (cm^{-1})	Raman $\Delta\nu_{vacuum}$ (cm^{-1})
$\nu_4{}^{CCl_2}(a_1)$	[143]	283 (s. pol.)[144]	$\nu_2+\nu_4(A_1)$	1548 (w.)	—
$\nu_3{}^{CCl}(a_1)$	704 (v.s.)[145]	700 (v.s. pol.)[144]	$\nu_3+\nu_7(B_1)$	1613 (w.)	—
$\nu_9{}^{CCl}(b_2)$	737 (v.s.)[145]	736 (s. depol.?)	$\nu_5+\nu_7(B_2)$	2057 (w.)	—
$\nu_7(b_1)$ (rocking)	899 (m.)	898 (v.w. depol.?)	$\nu_2+\nu_9(B_2)$	2136 (w.)	—
$\nu_3+\nu_4(A_1)$	935 (w.)	—	$\nu_2+\nu_7(B_1)$	2314 (m.)	—
$\nu_4+\nu_9(B_2)$?	1060 (w.)	1057 (v.w. pol.?)[146]	$\nu_5+\nu_8(B_1)$	2414 (w.)	—
$\nu_5(a_2)$?(torsion)	1155 (w.)	1148 (w. depol.)	$2\nu_8(A_1)$	2524 (w.)	—
$\nu_4+\nu_7(B_1)$	1192 (w.)	—	$\nu_2+\nu_8(B_2)$	2673 (w.)	
$\nu_3+2\nu_4(A_1)$?	1222 (w.)	—	$2\nu_2(A_1)$	—	2822 (v.w.)
$\nu_8(b_2)$ (rocking)	1266 (v.s.)	1255 (v.w.)	$\nu_1{}^{CH}(a_1)$	2984 (s.)	2985 (s. pol.)[144]
$\nu_2{}^{CH_2}(a_1)$	1429 (s.)	1417 (m. depol.)	$\nu_6{}^{CH}(b_1)$	3048 (s.)	3045 (s. depol.)
$2\nu_9(A_1)$	—	1464 (v.w.)	$4\nu_1$, $4\nu_6$?	11309 (v.w.)[147]	

[141] In addition, some very weak bands below 3049 and some weak bands above 3049 cm^{-1} have been found and assigned by Corin and Sutherland (233). Between 525 and 1450 cm^{-1} the absorption spectrum has also been measured, apparently under lower dispersion, by Lecomte (565) and Emschwiller and Lecomte (304).

[142] For somewhat different assignments see Corin and Sutherland (233) and Wu (25).

[143] Outside the region investigated, except in the work of Barchewitz and Parodi (101) on CH_2Cl_2 in paraffine solution. They give the bands 263, 500, 312, 222 cm^{-1} in the order of their intensities. It appears doubtful whether these bands belong to CH_2Cl_2.

[144] In the vapor, according to Nielsen and Ward (670), these lines occur at 280, 712, and 2997 cm^{-1},

[145] These two bands are due to Lecomte (565). Emschwiller and Lecomte (304) give 714 instead of 704.

[146] This band is not given by Wagner (908) but is given by both Trumpy (875) and Kohlrausch and Ypsilanti (534).

[147] This band was found by Timm and Mecke (864) and Vierling and Mecke (901) in the photographic infrared.

the fundamentals is still somewhat controversial. With one exception all infrared and Raman investigations refer to the liquid state.

As for CH_2D_2, there are nine fundamentals distributed over the various species as follows (see Tables 13 and 35):

$$4A_1 + A_2 + 2B_1 + 2B_2.$$

They are given qualitatively in Fig. 93, where it has been assumed that the CH_2 plane is the xz plane (parallel to the plane of the paper) and the two-fold axis the z axis. According to our experience with H_2CO and other molecules, we expect three vibrations characteristic of the CH_2 group (two symmetrical ones, a stretching and a deformation vibration, and one antisymmetrical stretching
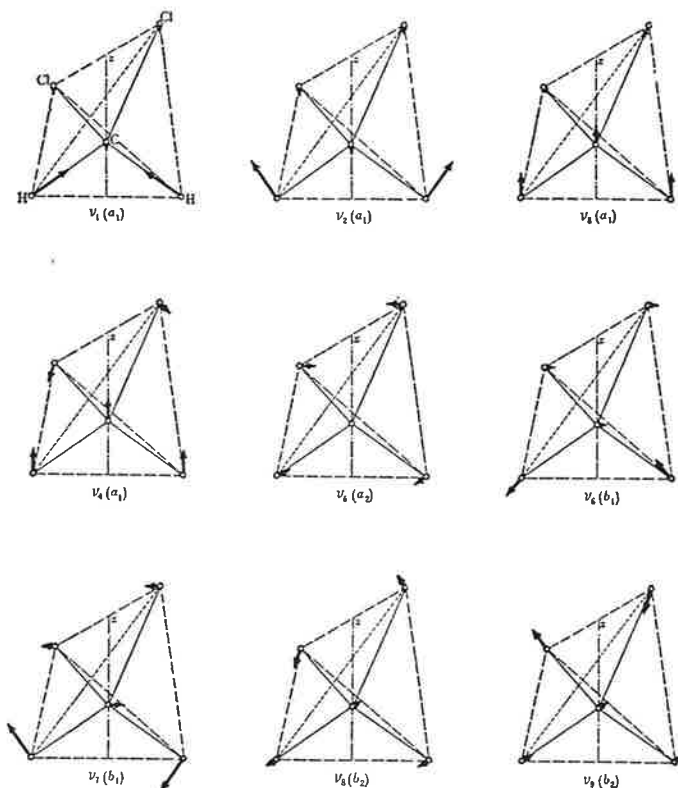
FIG. 93. Normal vibrations of CH_2Cl_2 (schematic).—The CH_2 plane is parallel, the CCl_2 plane perpendicular to the plane of the paper (shown in oblique projection). In ν_5, ν_8, ν_9 the H atoms move perpendicularly to the plane of the paper. In ν_5, ν_6, ν_7 the Cl atoms move perpendicularly to the CCl_2 plane, that is, parallel to the plane of the paper; in all others they move in the CCl_2 plane.

vibration) and three similar vibrations characteristic of the CCl_2 group. They are the vibrations $\nu_1(a_1)$, $\nu_2(a_1)$, $\nu_6(b_1)$ and $\nu_3(a_1)$, $\nu_4(a_1)$, $\nu_9(b_2)$ respectively of Fig. 93. This leaves the three vibrations $\nu_5(a_2)$, $\nu_7(b_1)$, and $\nu_8(b_2)$ which cannot be localized in a particular group. $\nu_5(a_2)$ is the torsion oscillation about the z axis mentioned previously (p. 240); ν_7 and ν_8 are the rocking vibrations of the CH_2 and CCl_2 groups respectively against the rest of the molecule.

All nine fundamentals are active in the Raman effect and all but $\nu_5(a_2)$ are active in the infrared. Table 87 gives the observed Raman and infrared bands. Five of the fundamentals are easily identified. The three lowest observed frequencies are obviously the three CCl_2 vibrations, since we know from the discussion of CCl_4, $HCCl_3$, and CH_3Cl that the C—Cl stretching vibration has a frequency of

about 700, and since the CCl_2 deformation frequency must be appreciably lower. This assignment also fits with the observed degrees of depolarization, only one of the three vibrations $[\nu_9(b_2)]$ being non-totally symmetric. Furthermore, it fits calculations assuming a valence force system in a triatomic system $Cl—CH_2—Cl$ [see Kohlrausch (14)]. The two high-frequency Raman shifts and infrared bands 2985 and 3047 cm^{-1} evidently are the C—H stretching frequencies of the CH_2 group: one, $\nu_1(a_1)$, totally symmetric and therefore polarized, and the other, $\nu_6(b_1)$, anti-symmetric with respect to the CCl_2 plane and therefore depolarized.

By comparison with the vibration spectra of H_2CO and the methyl halides, it would be expected that the fairly strong Raman and infrared band of CH_2Cl_2 at 1423 cm^{-1} would correspond to the CH_2 deformation vibration $\nu_2(a_1)$. Against this assignment the objection may be raised that in the Raman effect this frequency is completely depolarized, whereas $\nu_2(a_1)$ should be partly polarized. However, a very similar frequency has been observed in many other methylene compounds in which it is polarized [see Wagner (908)], and as has been pointed out earlier, polarized Raman lines may in exceptional cases have degrees of depolarization up to $\frac{6}{7}$.

The assignment of the three remaining frequencies $\nu_5(a_2)$ (torsional oscillation), $\nu_7(b_1)$ (rocking of CH_2 in its plane), $\nu_8(b_2)$ (rocking of CH_2 perpendicular to its plane) is much less certain. In Table 87 for ν_5 and ν_8 the assignment by Wagner (908) has been adopted; Wagner has carried out a detailed calculation on the basis of a somewhat generalized valence force system and has also compared CH_2Cl_2 with a number of other methylene compounds. The fact that $\nu_5(a_2)$ seems to occur (though weakly) in the infrared, contrary to the selection rules, must be explained as due to the influence of the neighboring molecules. It should not occur in the infrared spectrum of the vapor.[148] For $\nu_7(b_1)$ Wagner has left the assignment open, suggesting that ν_7 is overlapped by ν_9. In Table 87, following Corin and Sutherland (233), the frequency 898 cm^{-1} has been chosen for $\nu_7(b_1)$ since this is a fairly strong infrared band that cannot be explained as a combination or overtone band.
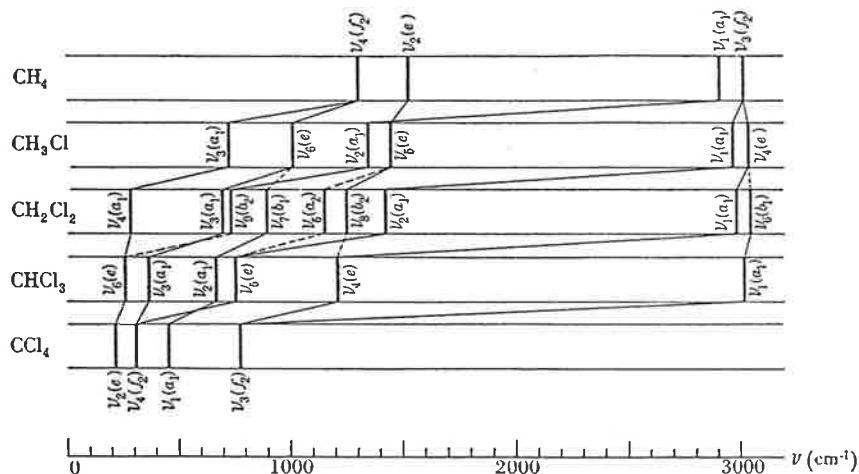

FIG. 94. Correlation of the fundamental vibrations of CH_4, CH_3Cl, CH_2Cl_2, $CHCl_3$, and CCl_4. —The broken correlation lines correspond to vibrations that are antisymmetric with respect to the (only) plane of symmetry that is preserved in going from CH_3Cl or from $CHCl_3$ to CH_2Cl_2.

The other observed infrared and Raman bands are easily assigned as overtone and combination bands, as indicated in Table 87.

In Fig. 94 the fundamental vibration spectra of CH_4, CH_3Cl, CH_2Cl_2, $CHCl_3$, CCl_4 are represented graphically on the basis of the data of Tables 80, 83, 84, 86, 87. Frequently in the literature attempts have been made to correlate the frequencies in these and similar molecules, but quite often such correlations have been made without regard for the non-crossing rule of vibrations of the same species (see p. 200). It must be realized that the correlation between CH_4 and CH_2Cl_2 is different

---

[148] Wu (962) assigns $\nu_5(a_2)$ to 898 cm^{-1} which seems much less likely since it occurs with medium intensity in the infrared.

depending on whether one imagines two of the H atoms of CH_4 to be simultaneously transformed into Cl atoms or whether one imagines first one H atom transformed into Cl (giving CH_3Cl) and then the other. In the first correlation there are throughout the transition two planes of symmetry, in the second only one. In the first case, therefore, intersections of vibrations of different species of C_{2v} may take place, whereas in the second case only vibrations of different species of the common point group C_s may intersect. This second case is the one represented in Fig. 94. In order to carry out this correlation one has to realize that the e vibrations of CH_3Cl split into one symmetric (a') and one antisymmetric (a'') vibration of C_s (indicated by solid and broken correlation lines respectively), while a_1 vibrations go over into a' vibrations. On the other hand, since it is the CCl_2 plane that remains a plane of symmetry, the a_1 and b_2 vibrations of CH_2Cl_2 go over into a' vibrations of C_s while a_2 and b_1 go over into a''. With this and the non-crossing rule, the correlation in the upper part of Fig. 94 is given. The correlation of CCl_4—$CHCl_3$—CH_2Cl_2 (lower part of Fig. 94) is similar, except that the plane in common is now the CH_2 plane; therefore a_1 and b_1 go over into a', and a_2 and b_2 into a''. Fig. 94 shows that in this correlation none of the vibrations of CH_4 goes over completely into the corresponding vibration of CCl_4. Kohlrausch and Wagner (531), as well as Wu (962), have given a correlation similar to Fig. 94 including as further intermediate steps CH_3D, CH_3F, CH_2FCl, $CHFCl_2$, $CDCl_3$, $CFCl_3$. However, their assignments for CH_2Cl_2 are slightly different from that assumed here.

$CHCl_2Br$ and $CHClBr_2$. A number of halogen derivatives of methane with two different halogens as well as hydrogen have been investigated in recent years, particularly by Glockler and his collaborators. As examples we choose bromodichloromethane and chlorodibromomethane. One would expect these molecules to have one plane of symmetry only (the CHBr and CHCl planes respectively), that is to belong to point group C_s. On this assumption each would be expected (see Table 35) to have six normal vibrations that are symmetric with respect to the plane of symmetry (species A') and three that are antisymmetric to it (species A''). All fundamentals are active both in the Raman

TABLE 88. COMPARISON OF THE FUNDAMENTALS OF $CHCl_3$, $CHCl_2Br$, $CHClBr_2$, AND $CHBr_3$ AS OBTAINED FROM THE RAMAN SPECTRA OF THE LIQUIDS.

Assignment	$CHCl_3$[149]	$CHCl_2Br$ [150]	$CHClBr_2$[150]	$CHBr_3$[151]
$\nu_6(e)$	262.0 (v.s.)	214.6 (s.) 220.4 (v.s.)	168.3 (s.) 201.1 (s.)	153.8 (s.)
$\nu_3(a_1)$	365.9 (s.)	329.6 (s.)	279.4 (v.s.)	222.3 (v.s.)
$\nu_2(a_1)$	668.3 (s.)	601.7 (s.)	568.9 (s.)	538.6 (s.)
$\nu_5(e)$	761.2 (s.)	718.8 (m.) 760.0 (m.)	658.7 (m.) 749.5 (m.)	656 (s.)
$\nu_4(e)$	1215.6 (m.)	1170.8 (m.) 1214.3 (w.)	1145.5 (w.) 1193.8 (w.)	1142 (m.)
$\nu_1(a_1)$	3018.9 (s.)	3020.5 (m.)	3022.6 (s.)	3023 (s.)

effect and in the infrared. The Raman spectra of liquid $CHCl_2Br$ and $CHClBr_2$ have been investigated by Kohlrausch and Köppl (522) and Glockler and Leader (374) (376), and the infrared spectrum of liquid $CHClBr_2$ by Emschwiller and Lecomte (304). For each molecule nine Raman shifts, which are presumably all fundamentals, have been found, and for $CHClBr_2$ four infrared bands which coincide within the rather large uncertainty of the measurements with four of the Raman shifts. Since no polarization data are available and the infrared data have been obtained with low dispersion, it is not possible to decide definitely which of the frequencies correspond to the antisymmetric vibrations.

However, a comparison of the spectra of $CHCl_2Br$ and $CHClBr_2$ with those of $CHCl_3$ and $CHBr_3$ is very helpful in finding out to what modes the observed frequencies of the former correspond, since to a certain very rough approximation $CHCl_2Br$ and $CHClBr_2$ may be considered as isotopic molecules of $CHCl_3$ in which one or two Cl atoms are replaced by Br, or of $CHBr_3$ in which

[149] From Table 86.

[150] These data are from Glockler and Leader (376).

[151] These data are from Redlich and Stricks (732).

two or one Br atoms are replaced by Cl atoms [see Wu (26)]. This comparison is given in Table 88. Here it should be noted that every degenerate vibration of $CHCl_3$ or $CHBr_3$ splits into two different frequencies in $CHCl_2Br$ and $CHClBr_2$, which one would expect to be intermediate in frequency between those of $CHCl_3$ and $CHBr_3$. This is seen to be the case from Table 88. One component of each such doublet is an antisymmetric vibration, but as mentioned above it is impossible at present to decide which one. The analogues of the totally symmetric vibrations of $CHCl_3$ and $CHBr_3$ also have, of course, intermediate frequencies.

It is seen from this comparison that while the three highest frequencies of $CHCl_2Br$ and $CHClBr_2$ may definitely be identified as C—H stretching and bending (rocking) vibrations it is not possible to ascribe any one of the others to a definite carbon-halogen band. One can say only that the three lowest are bending frequencies and that the three intermediate are stretching frequencies of the CCl_2Br and $CClBr_2$ groups.

Formic acid, HCOOH and HCOOD. The investigation of the infrared and Raman spectra of formic acid is complicated by the fact that at room temperature the vapor consists mainly of double molecules and only a small fraction of single molecules.[152] In order to ascertain which bands belong to the single molecules (and also to avoid too much overlapping by the bands of the double molecules), it is necessary to investigate the spectrum at an elevated temperature as well as at room temperature. This has been done for the infrared absorption by Bonner and Hofstadter (167) (455), both for light and heavy formic acid, and for the Raman spectrum of the former by Bonner and Kirby-Smith (168). The Raman spectrum of the liquid, investigated by many authors [see Kohlrausch (14)] is probably mostly due to the dimer. Table 89 gives a modern version of the frequencies of the fundamentals based on the papers by Millikan and Pitzer (1084) Reddington (1085) Hisatsune and Heicklen (1086) Bertie and Michaelian (1087) and Bertie et al. (1088) (see also vol. III).

TABLE 89. INFRARED AND RAMAN SPECTRA OF MONOMERIC HCOOH AND HCOOD VAPOR.

Assignment	HCOOH[155]	HCOOD
ν_7(OCO bend)a'	625.4	556.3
ν_9(OH tors)a″	641.8	507.5
ν_8(a″) CH wag	1033.4	1010.8
ν_6(a') C—O	1105.4	1177.7
ν_5(a') OH bend	1223.0	972.2
$2\nu_8$	1307 R $\Big\}$[156]	
ν_4(a') CH bend	1380.6 R	1368 R
ν_3(a') (C=O)	1776.2	1773.0
ν_2(a') (CH)	2943.8	2944
ν_1(a') OH(OD)	3570.0	2633.5

[152] For detailed data about the association equilibrium, see Coolidge (230).

[155] Two photographic infrared bands at 10202.8 and 13285 cm^{-1} have been observed by Herzberg and Verleger (445) Bauer and Badger (128) and Thompson (848).

[156] Fermi doublet (see (1087)).